

ENGINEERING OF BIOMATERIALS

INŻYNIERIA BIOMATERIAŁÓW

JOURNAL OF POLISH SOCIETY FOR BIOMATERIALS AND FACULTY OF MATERIALS SCIENCE AND CERAMICS AGH-UST

CZASOPISMO POLSKIEGO STOWARZYSZENIA BIOMATERIAŁÓW I WYDZIAŁU INŻYNIERII MATERIAŁOWEJ I CERAMIKI AGH

Number 155

Numer 155

Volume XXIII

Rok XXIII

APRIL 2020

KWIECIEŃ 2020

ISSN 1429-7248

PUBLISHER:

WYDAWCA:

**Polish Society
for Biomaterials
in Krakow**

Polskie
Stowarzyszenie
Biomateriałów
w Krakowie

**EDITORIAL
COMMITTEE:**

KOMITET

REDAKCYJNY:

Editor-in-Chief

Redaktor naczelny

Jan Chłopek

Editor

Redaktor

Elżbieta Pamuła

Secretary of editorial

Sekretarz redakcji

Design

Projekt

Katarzyna Trała

**ADDRESS OF
EDITORIAL OFFICE:**

ADRES REDAKCJI:

AGH-UST

30/A3, Mickiewicz Av.

30-059 Krakow, Poland

Akademia

Górniczno-Hutnicza

al. Mickiewicza 30/A-3

30-059 Kraków

Issue: 250 copies

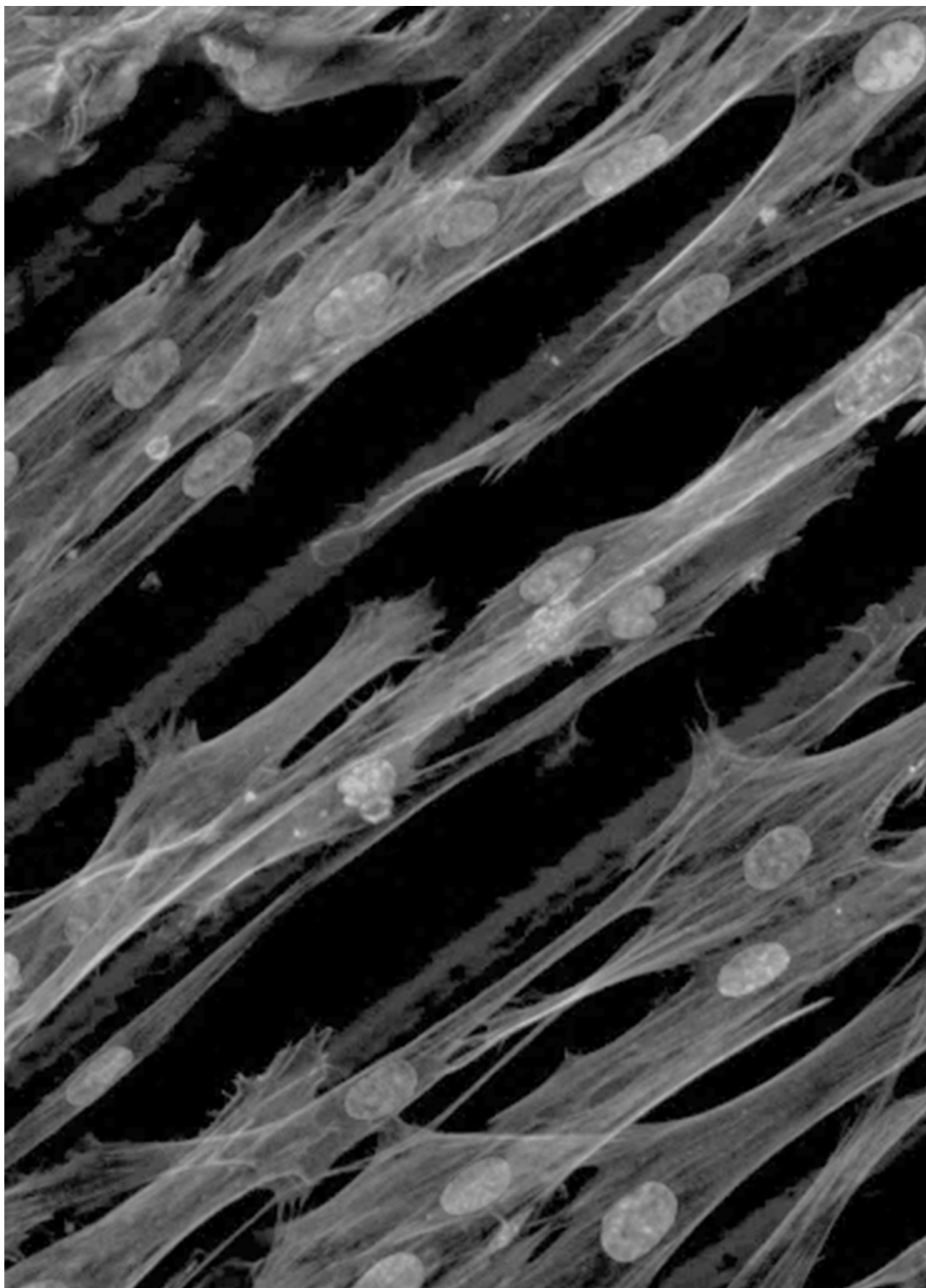
Nakład: 250 egz.

**Scientific Publishing
House AKAPIT**

Wydawnictwo Naukowe

AKAPIT

e-mail: wn@akapit.krakow.pl



**EDITORIAL BOARD
KOMITET REDAKCYJNY**

EDITOR-IN-CHIEF

Jan Chłopek - AGH UNIVERSITY OF SCIENCE AND TECHNOLOGY, KRAKOW, POLAND

EDITOR

Elżbieta Pamuła - AGH UNIVERSITY OF SCIENCE AND TECHNOLOGY, KRAKOW, POLAND

**INTERNATIONAL EDITORIAL BOARD
MIĘDZYNARODOWY KOMITET REDAKCYJNY**

Iulian Antoniac - UNIVERSITY POLITEHNICA OF BUCHAREST, ROMANIA

Lucie Bacakova - ACADEMY OF SCIENCE OF THE CZECH REPUBLIC, PRAGUE, CZECH REPUBLIC

Romuald Będziński - UNIVERSITY OF ZIELONA GÓRA, POLAND

Marta Błażewicz - AGH UNIVERSITY OF SCIENCE AND TECHNOLOGY, KRAKOW, POLAND

Stanisław Błażewicz - AGH UNIVERSITY OF SCIENCE AND TECHNOLOGY, KRAKOW, POLAND

Maria Borczuch-Łączka - AGH UNIVERSITY OF SCIENCE AND TECHNOLOGY, KRAKOW, POLAND

Wojciech Chrzanowski - UNIVERSITY OF SYDNEY, AUSTRALIA

Jan Ryszard Dąbrowski - BIAŁYSTOK TECHNICAL UNIVERSITY, POLAND

Timothy Douglas - LANCASTER UNIVERSITY, UNITED KINGDOM

Christine Dupont-Gillain - UNIVERSITÉ CATHOLIQUE DE LOUVAIN, BELGIUM

Matthias Epple - UNIVERSITY OF DUISBURG-ESSEN, GERMANY

Robert Hurt - BROWN UNIVERSITY, PROVIDENCE, USA

James Kirkpatrick - JOHANNES GUTENBERG UNIVERSITY, MAINZ, GERMANY

Ireneusz Kotela - CENTRAL CLINICAL HOSPITAL OF THE MINISTRY OF THE INTERIOR AND ADMINISTR. IN WARSAW, POLAND

Małgorzata Lewandowska-Szumieł - MEDICAL UNIVERSITY OF WARSAW, POLAND

Jan Marciniak - SILESIA UNIVERSITY OF TECHNOLOGY, ZABRZE, POLAND

Ion N. Mihailescu - NATIONAL INSTITUTE FOR LASER, PLASMA AND RADIATION PHYSICS, BUCHAREST, ROMANIA

Sergey Mikhalovsky - UNIVERSITY OF BRIGHTON, UNITED KINGDOM

Stanisław Mitura - TECHNICAL UNIVERSITY OF LIBEREC, CZECH REPUBLIC

Piotr Niedzielski - TECHNICAL UNIVERSITY OF LODZ, POLAND

Abhay Pandit - NATIONAL UNIVERSITY OF IRELAND, GALWAY, IRELAND

Stanisław Pielka - WROCLAW MEDICAL UNIVERSITY, POLAND

Vehid Salih - UCL EASTMAN DENTAL INSTITUTE, LONDON, UNITED KINGDOM

Jacek Składzień - JAGIELLONIAN UNIVERSITY, COLLEGIUM MEDICUM, KRAKOW, POLAND

Andrei V. Stanishevsky - UNIVERSITY OF ALABAMA AT BIRMINGHAM, USA

Anna Ślósarczyk - AGH UNIVERSITY OF SCIENCE AND TECHNOLOGY, KRAKOW, POLAND

Tadeusz Trzaska - UNIVERSITY SCHOOL OF PHYSICAL EDUCATION, POZNAŃ, POLAND

Dimitris Tsipas - ARISTOTLE UNIVERSITY OF THESSALONIKI, GREECE

Wskazówki dla autorów

1. Prace do opublikowania w kwartalniku „Engineering of Biomaterials / Inżynieria Biomateriałów” przyjmowane będą wyłącznie w języku angielskim.
2. Wszystkie nadsyłane artykuły są recenzowane.
3. Materiały do druku prosimy przysyłać za pomocą systemu online (www.biomaterials.pl).
4. Struktura artykułu:
 - TYTUŁ • Autorzy i instytucje • Streszczenie (200-250 słów) • Słowa kluczowe (4-6) • Wprowadzenie • Materiały i metody • Wyniki i dyskusja • Wnioski • Podziękowania • Piśmiennictwo
5. Autorzy przesyłają pełną wersję artykułu, łącznie z ilustracjami, tabelami, podpisami i literaturą w jednym pliku. Artykuł w tej formie przesyłany jest do recenzentów. Dodatkowo autorzy proszeni są o przesłanie materiałów ilustracyjnych (rysunki, schematy, fotografie, wykresy) w oddzielnych plikach (format np. .jpg, .gif, .tiff, .bmp). Rozdzielczość rysunków min. 300 dpi. Wszystkie rysunki i wykresy powinny być czarno-białe lub w odcieniach szarości i ponumerowane cyframi arabskimi. W tekście należy umieścić odnośniki do rysunków i tabel. W przypadku artykułów dwujęzycznych w tabelach i na wykresach należy umieścić opisy polskie i angielskie.
6. Na końcu artykułu należy podać wykaz piśmiennictwa w kolejności cytowania w tekście i kolejno ponumerowany.
7. Redakcja zastrzega sobie prawo wprowadzenia do opracowań autorskich zmian terminologicznych, poprawek redakcyjnych, stylistycznych, w celu dostosowania artykułu do norm przyjętych w naszym czasopiśmie. Zmiany i uzupełnienia merytoryczne będą dokonywane w uzgodnieniu z autorem.
8. Opinia lub uwagi recenzentów będą przekazywane Autorowi do ustosunkowania się. Nie dostarczenie poprawionego artykułu w terminie oznacza rezygnację Autora z publikacji pracy w naszym czasopiśmie.
9. Za publikację artykułów redakcja nie płaci honorarium autorskiego.
10. Adres redakcji:
Czasopismo
„Engineering of Biomaterials / Inżynieria Biomateriałów”
Akademia Górniczo-Hutnicza im. St. Staszica
Wydział Inżynierii Materiałowej i Ceramiki
al. Mickiewicza 30/A-3, 30-059 Kraków
tel. (48) 12 617 25 03, 12 617 25 61
tel./fax: (48) 12 617 45 41
e-mail: chlopek@agh.edu.pl, kabe@agh.edu.pl

Szczegółowe informacje dotyczące przygotowania manuskryptu oraz procedury recenzowania dostępne są na stronie internetowej czasopisma:
www.biomaterials.pl

Warunki prenumeraty

Zamówienie na prenumeratę prosimy przysyłać na adres:
mgr inż. Augustyn Powroźnik
apowroz@agh.edu.pl, tel/fax: (48) 12 617 45 41
Cena pojedynczego numeru wynosi 20 PLN
Konto: Polskie Stowarzyszenie Biomateriałów
30-059 Kraków, al. Mickiewicza 30/A-3
ING Bank Śląski S.A. O/Kraków
nr rachunku 63 1050 1445 1000 0012 0085 6001

Prenumerata obejmuje 4 numery regularne i nie obejmuje numeru specjalnego (materiały konferencyjne).

Instructions for authors

1. Papers for publication in quarterly journal „Engineering of Biomaterials / Inżynieria Biomateriałów” should be written in English.
2. All articles are reviewed.
3. Manuscripts should be submitted to editorial office through online submission system (www.biomaterials.pl).
4. A manuscript should be organized in the following order:
 - TITLE • Authors and affiliations • Abstract (200-250 words) • Keywords (4-6) • Introduction • Materials and Methods • Results and Discussions • Conclusions • Acknowledgements • References
5. All illustrations, figures, tables, graphs etc. preferably in black and white or grey scale should be additionally sent as separate electronic files (format .jpg, .gif, .tiff, .bmp). High-resolution figures are required for publication, at least 300 dpi. All figures must be numbered in the order in which they appear in the paper and captioned below. They should be referenced in the text. The captions of all figures should be submitted on a separate sheet.
6. References should be listed at the end of the article. Number the references consecutively in the order in which they are first mentioned in the text.
7. The Editors reserve the right to improve manuscripts on grammar and style and to modify the manuscripts to fit in with the style of the journal. If extensive alterations are required, the manuscript will be returned to the authors for revision.
8. Opinion or notes of reviewers will be transferred to the author. If the corrected article will not be supplied on time, it means that the author has resigned from publication of work in our journal.
9. Editorial does not pay author honorarium for publication of article.
10. Address of editorial office:
Journal
„Engineering of Biomaterials / Inżynieria Biomateriałów”
AGH University of Science and Technology
Faculty of Materials Science and Ceramics
30/A-3, Mickiewicz Av., 30-059 Krakow, Poland
tel. (48) 12) 617 25 03, 12 617 25 61
tel./fax: (48) 12 617 45 41
e-mail: chlopek@agh.edu.pl, kabe@agh.edu.pl

Detailed information concerning manuscript preparation and review process are available at the journal's website:
www.biomaterials.pl

Subscription terms

Contact:
MSc Augustyn Powroźnik,
e-mail: apowroz@agh.edu.pl
Subscription rates:
Cost of one number: 20 PLN
Payment should be made to:
Polish Society for Biomaterials
30/A3, Mickiewicz Av.
30-059 Krakow, Poland
ING Bank Śląski S.A.
account no. 63 1050 1445 1000 0012 0085 6001

Subscription includes 4 issues and does not include special issue (conference materials).

●●●●●●●●●●●●●●●●●●

STUDIA PODYPLOMOWE

Biomateriały – Materiały dla Medycyny

2020/2021

<p>Organizator: Akademia Górniczo-Hutnicza im. Stanisława Staszica w Krakowie Wydział Inżynierii Materiałowej i Ceramiki Katedra Biomateriałów i Kompozytów</p> <p>Kierownik: prof. dr hab. inż. Elżbieta Pamuła Sekretarz: dr inż. Małgorzata Krok-Borkowicz</p>	<p>Adres: 30-059 Kraków, Al. Mickiewicza 30 Pawilon A3, p. 208, 210 lub 501 tel. 12 617 44 48, 12 617 23 38, fax. 12 617 33 71 email: epamula@agh.edu.pl; krok@agh.edu.pl</p> <p>https://www.agh.edu.pl/ksztalcenie/oferta-ksztalcenia/studia-podyplomowe-kursy-dokształcające-i-szkolenia/biomateriały-materiały-dla-medycyny/</p>
<p>Charakterystyka: Tematyka prezentowana w trakcie zajęć obejmuje przegląd wszystkich grup materiałów dla zastosowań medycznych: metalicznych, ceramicznych, polimerowych, węglowych i kompozytowych. Słuchacze zapoznają się z metodami projektowania i wytwarzania biomateriałów a następnie możliwościami analizy ich właściwości mechanicznych, właściwości fizykochemicznych (laboratoria z metod badań: elektronowa mikroskopia skaningowa, mikroskopia sił atomowych, spektroskopia w podczerwieni, badania energii powierzchniowej i zwilżalności) i właściwości biologicznych (badania: <i>in vitro</i> i <i>in vivo</i>). Omawiane są regulacje prawne i aspekty etyczne związane z badaniami na zwierzętach i badaniami klinicznymi (norma EU ISO 10993). Słuchacze zapoznają się z najnowszymi osiągnięciami w zakresie nowoczesnych nośników leków, medycyny regeneracyjnej i inżynierii tkankowej.</p>	
<p>Sylwetka absolwenta: Studia adresowane są do absolwentów uczelni technicznych (inżynieria materiałowa, technologia chemiczna), przyrodniczych (chemia, biologia, biotechnologia) a także medycznych, stomatologicznych, farmaceutycznych i weterynaryjnych, pragnących zdobyć, poszerzyć i ugruntować wiedzę z zakresu inżynierii biomateriałów i nowoczesnych materiałów dla medycyny. Słuchacze zdobywają i/lub pogłębiają wiedzę z zakresu inżynierii biomateriałów. Po zakończeniu studiów wykazują się znajomością budowy, właściwości i sposobu otrzymywania materiałów przeznaczonych dla medycyny. Potrafią analizować wyniki badań i przekładać je na zachowanie się biomateriału w warunkach żywego organizmu. Ponadto słuchacze wprowadzani są w zagadnienia dotyczące wymagań normowych, etycznych i prawnych niezbędnych do wprowadzenia nowego materiału na rynek. Ukończenie studiów pozwala na nabycie umiejętności przygotowywania wniosków do Komisji Etycznych i doboru metod badawczych w zakresie analizy biogodności materiałów.</p>	
<p>Zasady naboru: Termin zgłoszeń: od 20.09.2020 do 20.10.2020 (liczba miejsc ograniczona - decyduje kolejność zgłoszeń) Wymagane dokumenty: dyplom ukończenia szkoły wyższej Osoby przyjmujące zgłoszenia: prof. dr hab. inż. Elżbieta Pamuła (pawilon A3, p. 208, tel. 12 617 44 48, e-mail: epamula@agh.edu.pl) dr inż. Małgorzata Krok-Borkowicz (pawilon A3, p. 210, tel. 12 617 23 38, e-mail: krok@agh.edu.pl)</p>	
<p>Czas trwania: 2 semestry (od XI 2020 r. do VI 2021 r.) 8 zjazdów (soboty-niedziele) 1 raz w miesiącu</p>	<p>Opłaty: 2 600 zł (za dwa semestry)</p>



29th Biomaterials in Medicine and Veterinary Medicine Annual Conference

15 – 18 October 2020 Rytro, Poland

SAVE THE DATE

15-18

OCTOBER
2020

www.biomat.agh.edu.pl



REGISTER
AND
SUBMIT
AN ABSTRACT



SPIS TREŚCI CONTENTS

**DOUBLE CROSSLINKING OF CHITOSAN/
VANILLIN HYDROGELS AS A BASIS FOR
MECHANICALLY STRONG GRADIENT
SCAFFOLDS FOR TISSUE ENGINEERING**
MARTYNA HUNGER, PATRYCJA DOMALIK-
PYZIK, KATARZYNA RECZYŃSKA,
JAN CHŁOPEK 2

**PREPARATION AND CHARACTERIZATION
OF BIO-HYBRID HYDROGEL MATERIALS**
DAGMARA MALINA, EWELINA KRÓLICKA,
KATARZYNA BIALIK-WĄS, KLAUDIA PLUTA 12

ORGANIC BACTERIOSTATIC MATERIAL
TOMASZ FLAK, JAROSŁAW PALUCH,
JADWIGA GABOR, HUBERT OKŁA,
ARKADIUSZ STANULA, JAROSŁAW
MARKOWSKI, JAN PILCH,
ANDRZEJ SZYMON SWINAREW 17

**LASER MODIFIED FUNCTIONAL
CARBON-BASED COATINGS ON TITANIUM
SUBSTRATE FOR CARDIAC TISSUE
INTEGRATION AND BLOOD CLOTTING
INHIBITION**
ROMAN MAJOR, ROMAN OSTROWSKI,
MARCIN SURMIAK, KLAUDIA TREMBECKA-
WÓJCIGA, JUERGEN LACKNER 22

DOUBLE CROSSLINKING OF CHITOSAN/VANILLIN HYDROGELS AS A BASIS FOR MECHANICALLY STRONG GRADIENT SCAFFOLDS FOR TISSUE ENGINEERING

MARTYNA HUNGER* , PATRYCJA DOMALIK-PYZIK ,
KATARZYNA RECZYŃSKA , JAN CHŁOPEK 

DEPARTMENT OF BIOMATERIALS AND COMPOSITES,
FACULTY OF MATERIALS SCIENCE AND CERAMICS,
AGH UNIVERSITY OF SCIENCE AND TECHNOLOGY,
MICKIEWICZ AVE. 30, 30-059 KRAKOW, POLAND
*E-MAIL: HUNGER@AGH.EDU.PL

Abstract

Polysaccharides, such as chitosan (CS), are widely used in many biomedical applications. However, they require crosslinking agents to achieve chemical stability and appropriate mechanical properties. In this work, chitosan-based hydrogels were crosslinked using vanillin and/or sodium tripolyphosphate, as chemical and physical crosslinking agents, respectively. Microstructural (digital microscope, SEM), structural (FTIR-ATR), mechanical (static compression test), and in vitro biological (chemical stability and swelling ratio in PBS, cytotoxicity) properties of the obtained materials were evaluated to assess materials potential as biomedical scaffolds. The optimal ratio of vanillin to chitosan (DD = 89%) to crosslink the polymer was found to be 1.2:1. Moreover, the double crosslinking with vanillin caused a two-time increase in the compression strength of the samples and led to the slower biodegradability. Cytotoxicity studies showed that the cells prefer double vanillin crosslinked hydrogels over those treated with TPP. Further studies, such as bioactivity are required to determine the specific functionality of the hydrogels and the specific tissue which may be treated with the tested materials. The optimal material was chosen to the next step of the study, which may be obtaining composite hydrogels with hydroxyapatite and/or graphene oxide to tailor or improve properties towards specific tissue regeneration.

Keywords: hydrogel, chitosan, vanillin, tripolyphosphate, tissue engineering

[Engineering of Biomaterials 155 (2020) 2-11]

doi:10.34821/eng.biomat.155.2020.2-11

Introduction

Polysaccharides, a large group of natural polymers such as chitosan (CS), hyaluronic acid (HA), alginates, gellan gum (GG) have been widely used to form hydrogels for tissue engineering applications. CS seems to be one of the most versatile among them [1]. Its polycationic nature and the presence of amino groups allow to form biocompatible scaffolds which are able to absorb large amounts of water and are prone to further modifications. Thus, CS-based systems mimicking many native tissues may be created for the regeneration of skin [2,3], bone [4,5], cartilage [6,7], nerves [8], or blood vessels [9].

There are many different ways to crosslink CS and thus form chemically stable and mechanically strong hydrogels, i.e. chemical, physical or metal-coordination-based crosslinking [10]. Chemically formed networks are created using dialdehydes, e.g. glutaraldehyde, yet most of them are considered cytotoxic. Genipin is a natural non-toxic agent which has also been widely used. As a crosslinking agent for CS, it improves the cell viability on hydrogels. However, the conditions of the crosslinking reaction influence the hydrogel structure significantly [11]. Another natural aldehyde, not only cyto-compatible but also much cheaper, is vanillin. There is evidence that vanillin improves the mechanical properties of the chitosan hydrogel [12]. Moreover, it is an antioxidant, which constitutes its significant advantage [13]. As a CS crosslinker, it is mainly used to obtain films [14], membranes [15] or drug microcarriers and microspheres [16,17]. However, the insufficient chemical stability of hydrogels crosslinked with vanillin requires additional modifications to prevent the CS matrix from being altered immediately after its generation.

The main disadvantage of covalent crosslinking is the chemical selectivity of the process which may lead to producing toxic side-products. Moreover, the limited control over the created microstructure makes this crosslinking method less desirable [18]. The click-chemistry reaction may be a more preferable solution but only a functionalized CS may be used to prepare hydrogels through this reaction [19]. The same limitation occurs when CS is crosslinked enzymatically, which makes these methods impractical [20].

Forming coordination complexes based on the reaction between amine or hydroxyl groups of CS and metal ions is yet another method to obtain the CS-based hydrogel. Although it is a quick process, the final crosslinked polymer is characterized by lower stability. In addition, this method is very sensitive to changes of the polysaccharide properties [21].

The physically crosslinked CS hydrogel is the result of forming CS polycations and electrostatic interactions with oppositely charged molecules. Ionic crosslinking may provide a decrease in the swelling ratio of the final hydrogel, dependant on the pH value [22]. One of the physical crosslinking agents used for CS is tripolyphosphate (TPP) [24]. This crosslinker is cyto-compatible and the final properties of CS-based hydrogel are easily tailorable, for example by different crosslinking degrees. On the other hand, the mechanical properties of physically crosslinked hydrogels are relatively low. In addition, thus obtained hydrogel exhibits a fast biodegradability [23-25] while, in bone tissue engineering scaffolds are required to be mechanically strong and stable under physiological conditions.

One of the solutions to improve the chemical stability and mechanical characteristic of the hydrogel is to apply the second crosslinking, which may increase both the hydrogel biodegradability and mechanical strength, due to the presence of additional bonds and a more tangled network. Additionally, using a natural crosslinking agent provides higher biocompatibility, therefore a combination of two crosslinking mechanisms may significantly improve the hydrogel properties [17].

This study involved a double-step crosslinking process for chitosan, based on chemical (vanillin) and/or physical (TPP) crosslinking. A natural polysaccharide, such as chitosan, and a natural crosslinking agent, such as vanillin were applied to improve the biocompatibility of the final hydrogel. Co-acting of the chemical and/or physical crosslinking reactions were studied to improve the mechanical properties and slow down biodegradation in the physiological environment.

Materials and Methods

Materials

Chitosan (CS; Mw = 100.000-300.000) was purchased from Acros Organics, USA. Avantor Performance Materials Poland S.A. reagents were used as follows: acetic acid (AAc; 99.9%), vanillin, sodium tripolyphosphate (TPP) and ethanol (EtOH; 96%). First, CS and vanillin powders were dissolved in 2% AAc and EtOH, respectively. As the first crosslinking step, the appropriate VAN solutions (1 ml) were added dropwise to the CS, mixed vigorously and homogenized by sonication (10 min). The final concentration of CS solution was controlled at 5% w/v of the final volume (20 ml). The mass ratios of CS:VAN and final concentrations of VAN are presented in TABLE 1. After mixing, the samples were left at room temperature and subsequently tested after 3, 4, 5 and 6 days of crosslinking. The 6x6 mm cubic samples of 1van, 1.2van, 1.4van were initially crosslinked with vanillin and maintained for 6 days. For the second crosslinking step they were cut and immersed in a vanillin solution (5% in EtOH, denoted as VAN_1, VAN_1.2, VAN_1.4) or a TPP solution (5% in distilled water, denoted as TPP_1, TPP_1.2, TPP_1.4) for 24 h to improve the crosslinking process. The proportion of hydrogel mass to crosslinking solution volume was 1g:10ml. Some of the samples were frozen at -80°C and freeze-dried for further analysis.

TABLE 1. The mass ratios of CS:VAN used in the study.

CS:VAN mass ratio	1:0.8	1:1	1:1.2	1:1.4	1:1.6
Sample description	0.8van	1van	1.2van	1.4van	1.6van
Final concentration of VAN [%]	4	5	6	7	8

Methods

Determination of a deacetylation degree (DD)

The deacetylation degree of chitosan used in this study was determined using the titration method [26]. Briefly, CS powder (0.2 g) dissolved in 0.1M HCl (20 ml) and deionized water (50 ml) was titrated with 0.1M NaOH. The pH changes dependent on titrant volume allowed to carry out the calculation using Formula 1:

$$DD = 2.03 \cdot \frac{V_2 - V_1}{m + 0.0042(V_2 - V_1)} \cdot 100\% \quad (1)$$

where: m – the exact mass of CS powder [g], V_1 and V_2 – volumes of 0.1M NaOH solution corresponding to the deflection points [ml], 2.03 – coefficient resulting from the molecular weight of chitin monomer unit, 0.0042 – coefficient connected with the difference between molecular weights of chitin and chitosan monomer units.

Chemical stability test

The biodegradation *in vitro* process was carried out in the PBS (Phosphate-Buffered Saline, pH = 7.4) solution at 37°C. The ratio of the sample mass to the PBS solution volume was 1g:100ml. The following time points were tested: 1, 2, 3, 4, 5, 6, 7, 14, 21 and 28 days. After the first 7 days of incubation, the PBS solution was substituted with the fresh one. At these intervals, the pH value was measured. After 28 days of incubation, the samples were washed with distilled water and weighed. The weight loss (WL) was calculated using Formula 2:

$$WL = \frac{M_0 - M_j}{M_0} \cdot 100 [\%] \quad (2)$$

where: M_0 – the initial mass of the sample [g], M_j – the weight of the sample after 28 days of incubation [g]

Static compression test

The universal testing machine (Zwick 1435, Germany) was used to analyze the mechanical properties of the samples (static compression test). All the measurements were performed using wet cubic samples, at room temperature. The samples after 28 days of incubation were also tested (denoted as: VAN_1_PBS, VAN_1.2_PBS, VAN_1.4_PBS, TPP_1_PBS, TPP_1.2_PBS, TPP_1.4_PBS). The Young's modulus and compressive strength values (at 3 mm deformation) were evaluated; Young's modulus was determined based on a linear fragment of the stress-strain curve. The strain was evaluated at F=10N and the stress was measured at 3 mm of strain. The test speed was set on 2 mm/min.

Swelling ratio

The samples were weighed and immersed in the PBS solution at 37°C. The swelling ratios were assessed after 1, 2, 3, 4 and 5 hours of the incubation, and then daily up to the 5th day. At these points, the swollen samples were dried carefully with a tissue, then weighed and placed back in the PBS solutions. The calculations of swelling ratio (SR) were made using Formula 3:

$$SR = \frac{M_i - M_0}{M_0} \cdot 100 [\%] \quad (3)$$

where: M_i – the weight of the swollen sample [g], M_0 – the initial mass of the sample [g]

Cytotoxicity test *in vitro*

The cytotoxicity studies were conducted using extracts in accordance with the ISO norm 10993-5 (2009). The materials were tested in contact with osteoblastogenic cells of the MG-63 line (European Cell Bank - European Collection of Cell Cultures, Salisbury, UK). The cells were cultured in the EMEM medium (Eagle's Minimal Essential Medium, PAN BIOTECH, Germany) with the addition of 10% bovine serum (Fetal Bovine Serum, Biowest, France) and 1% antibiotics (penicillin/streptomycin, PAA, Austria), 0.1% amino acids and 0.1% pyruvate (PAA, Austria). The culture was carried out at 37°C, 5% CO₂ and under the increased humidity.

The extraction was performed based on the 100 mg:1 ml ratio of the tested material to the culture medium. The weighed freeze-dried samples were immersed in the culture medium (the exact masses and volumes are summarized in TABLE 2) and left for 24 h at 37°C. Then the extracts were sterilized via filtration using syringe filters (0.22 μm).

TABLE 2. Samples tested on extracts, the exact sample weights and medium volumes used for extraction.

Sample	Mass [mg]	Culture medium volume [ml]
VAN_1	423.23	4.230
VAN_1.2	426.60	4.265
VAN_1.4	423.05	4.230
TPP_1	433.07	4.330
TPP_1.2	416.32	4.165
TPP_1.4	416.27	4.165
Medium	-	4.000

The following dilutions of extracts were prepared in the study: 1 (undiluted), 1/2, 1/4, 1/8 and 1/16. The culture medium was used to dilute the extracts. As the reference sample served the culture medium maintained under the conditions identical to the ones of the tested samples (no dilutions were used for the medium).

The cells were placed in 96-well plates - 5,000 cells per well (100 μ l medium). After 24 h of incubation, the supernatant medium was replaced with the appropriately diluted extracts (100 μ l). After the next 24 h, cell metabolic activity and viability were tested using the AlamarBlue test and live/dead staining. For this purpose, the following chemicals and devices were used: In Vitro Toxicology Assay Kit, resazurin-based (Sigma Aldrich), calcein AM/propidium iodide (Sigma Aldrich), Zeiss Axiovert 40 fluorescence microscope (Carl Zeiss, Germany) and BMG Labtech spectrofluorimeter, FluoStar Omega.

The calculations of resazurin reduction (RR) were made by Formula 4:

$$RR [\%] = \frac{F_{\text{sample}} - F_{0\% \text{ red}}}{F_{100\% \text{ red}} - F_{0\% \text{ red}}} \cdot 100\% \quad (4)$$

where: F_{sample} - fluorescence of sample from culture well, $F_{0\% \text{ red}}$ - fluorescence of culture medium with the addition of AlamarBlue reagent without cells, $F_{100\% \text{ red}}$ - fluorescence of culture medium with the addition of AlamarBlue reagent reduced of 100% by autoclaving (15 min, 121°C).

The statistical analysis was performed using ANOVA (One Way Analysis of Variance) followed by Tukey post-hoc test. The significance levels were set at $p < 0.05$ and $p < 0.001$. The normality and equal variances were tested with the Shapiro-Wilk and Leuven test, respectively, at $p < 0.05$.

Results and Discussion

The charts presenting the results after the CS powder titration are shown in FIG. 1. Based on the pH dependence on the NaOH volume added to the CS solution, the deacetylation degree of chitosan used was determined. After the calculation using Formula 1 the DD was found to be 89%. This parameter determined the CS properties, such as a susceptibility to modifications, the availability of the functional amino groups and solubility. It also possibly changed the crosslinking degree, thus influencing the mechanical properties or chemical stability. It is worth noting that the higher DD is desirable regarding the hydrogels applicability in tissue engineering. The obtained DD = 89% of the tested chitosan provided its good solubility and increased access to free amino groups, thus making the material more reactive to crosslinking process [27-29].

The obtained CS solutions before and after the single crosslinking process (after 3 days) are shown in FIG. 2. The addition of VAN solution caused an immediate colour change. This indicated the beginning of the reaction forming Schiff-base between the CS amino groups and the VAN aldehyde groups, as well as hydrogen bonds between both hydroxyl groups [30]. The higher the mass ratio of CS:VAN was, the more immediate the crosslinking process. In the 1.6van case, the solution viscosity was visibly higher after just one minute of mixing. The structure bonded more quickly and externally more strongly, thus blocking the access to the material's deeper parts, which resulted in the insufficient crosslinking and the non-homogenous structure. Although mechanical properties increased with the increased amount of crosslinking agent, the chemical stability decreased [31].

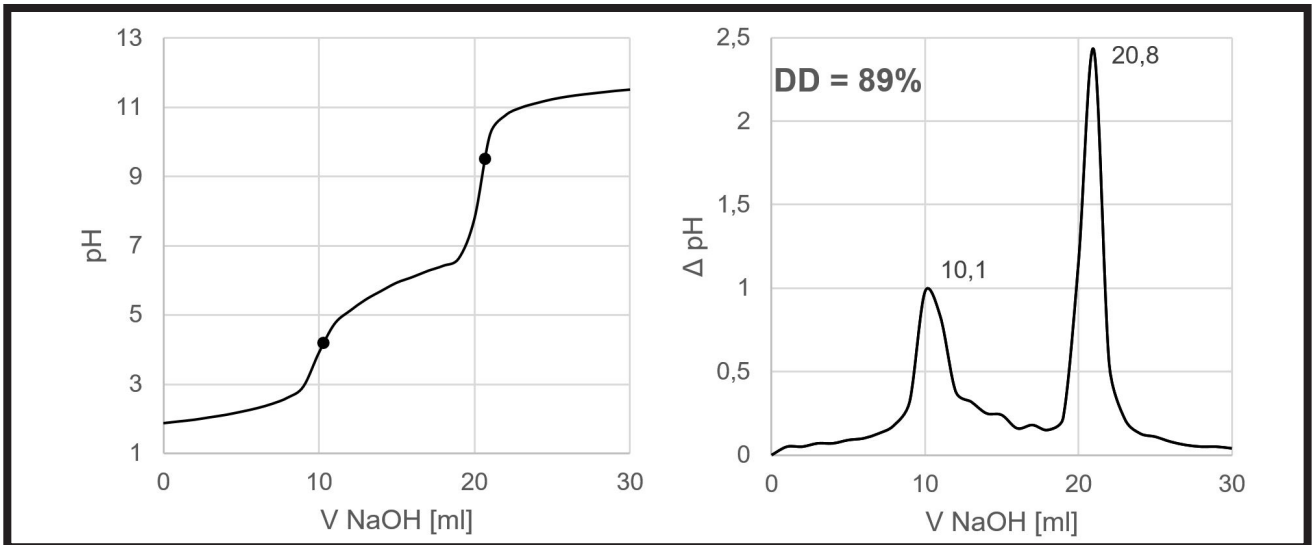


FIG. 1. The results of titration for CS powder – determination of deacetylation degree.



FIG. 2. The obtained samples before (left) and after (right) the single crosslinking, according to increasing mass ratio of VAN:CS.

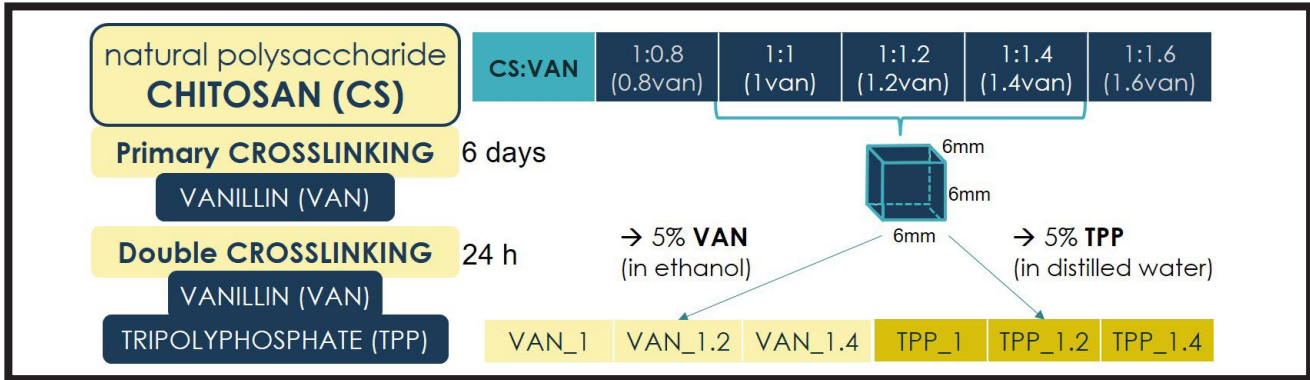


FIG. 3. The scheme of preparing the double crosslinked samples.

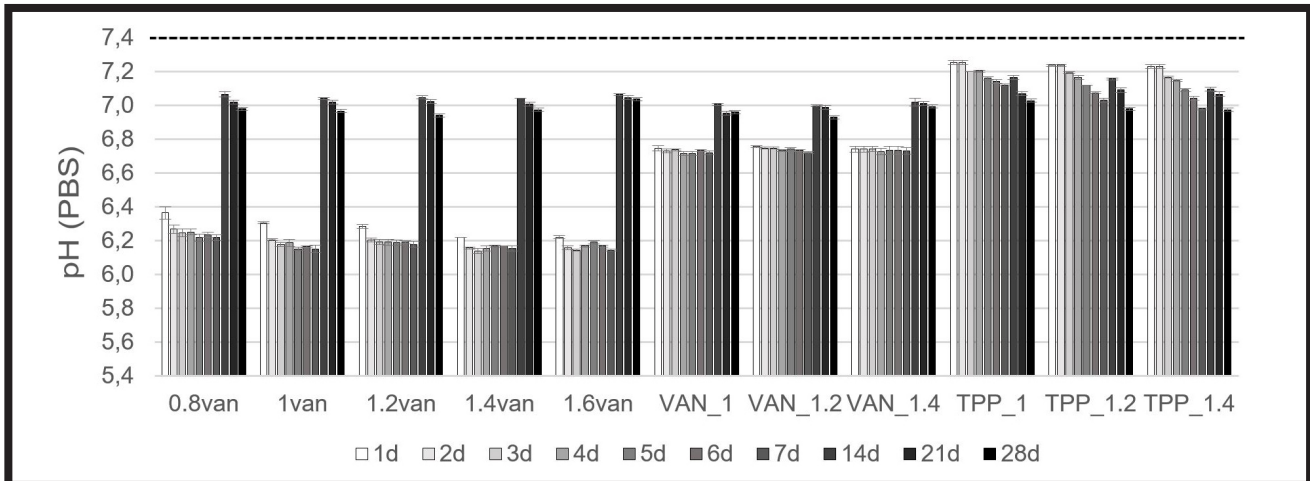


FIG. 4. The chemical stability test results – pH changes of incubation medium (PBS); triplets were tested for each type of material; error bars present standard deviations.

The scheme of double crosslinked materials preparation is presented in FIG. 3. The prepared cubic samples were maintained in the VAN or TPP solution for 24 h and then washed with distilled water for further studies. The TPP addition led to the formation of an ionically crosslinked hydrogel network, thus changing its properties [32].

The samples chemical stability was evaluated via the *in vitro* incubation test carried out in the PBS solution. The changes in the pH of the incubation media are presented in FIG. 4. The results indicated higher chemical stability of the double VAN-crosslinked samples, as compared to the single crosslinked CS. An initial pH decrease was caused by washing out the residual acetic acid or the non-crosslinked chitosan cations. However, the double VAN-crosslinked and TPP-crosslinked samples provided the initial pH at a higher level of about 6.7 and 7.2, respectively. The TPP addition in the hydrogel did not acidify the PBS solution significantly. Due to its alkaline nature [33], it provided better pH compatibility with human physiological fluids. However, for the TPP sample, its pH decreased with the incubation time as compared to the VAN-crosslinked sample where pH remained relatively constant both before and after the PBS substitution. Singh *et al.* provided evidence that the pH decrease and the lower oxygen level (2%) may affect cell viability and chondrogenesis [34]. The observations after 4 days of the cell culture pointed a decreased cell viability at pH = 6.2; the effect was not observed at pH = 7.2. Moreover, the alkaline environment seemed to be more beneficial for osteogenesis [35].

The results suggested that the double-crosslinked hydrogel network was more interconnected, the additional bonds formed and the stable structure was created. This initial effect was reduced after the PBS solution was substituted with the fresh one. This suggests that a longer pre-incubation period is required before testing the materials, for example in biological studies.

The weight loss results (FIG. 5) indicated that the double VAN-crosslinked samples exhibited the slowest degradation rate. The VAN_1, VAN_1.2 and VAN_1.4 samples after 4 weeks of the PBS incubation lost only around 5 % of their initial weight, while for the double TPP-crosslinked samples the weight loss was over twice as high. The weight loss of the single crosslinked samples was of 14-34%. In addition, starting with 1van, the more vanillin was in the material, the higher weight loss was observed. As mentioned above, the higher crosslinking agent/chitosan mass ratio was the more insufficient crosslinking occurred - as the non-crosslinked parts of the polymer dissolved and got released in the PBS solution. This phenomenon suggested that the optimal proportion of CS:VAN to crosslink the material in the first step would be 1:1. The second step of improving the crosslinked network provided a significantly more stable chemical structure, thus reducing the mass loss and slowing down the degradation process.

In general, it is necessary to apply chemically stable scaffolds to effectively repair tissue damages, otherwise, the regeneration process may be incomplete and new defects may occur. Therefore, it is vital to provide a relatively stable scaffold which may support tissue regeneration for minimum 3 months. During this period the scaffold integrates with the material and then the new tissue fills the defect. Moreover, the applied scaffold should degrade within 1 year [36,37].

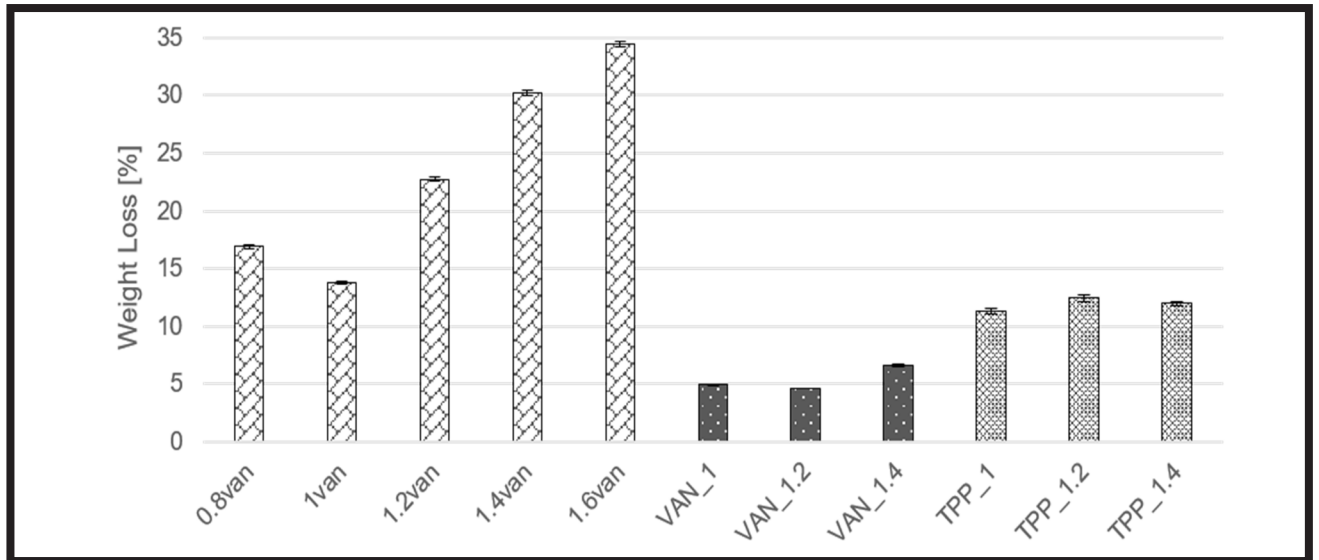


FIG. 5. The chemical stability test results – weight loss after 28 days of incubation in PBS solution; triplets were tested for each type of material; error bars present standard deviations.

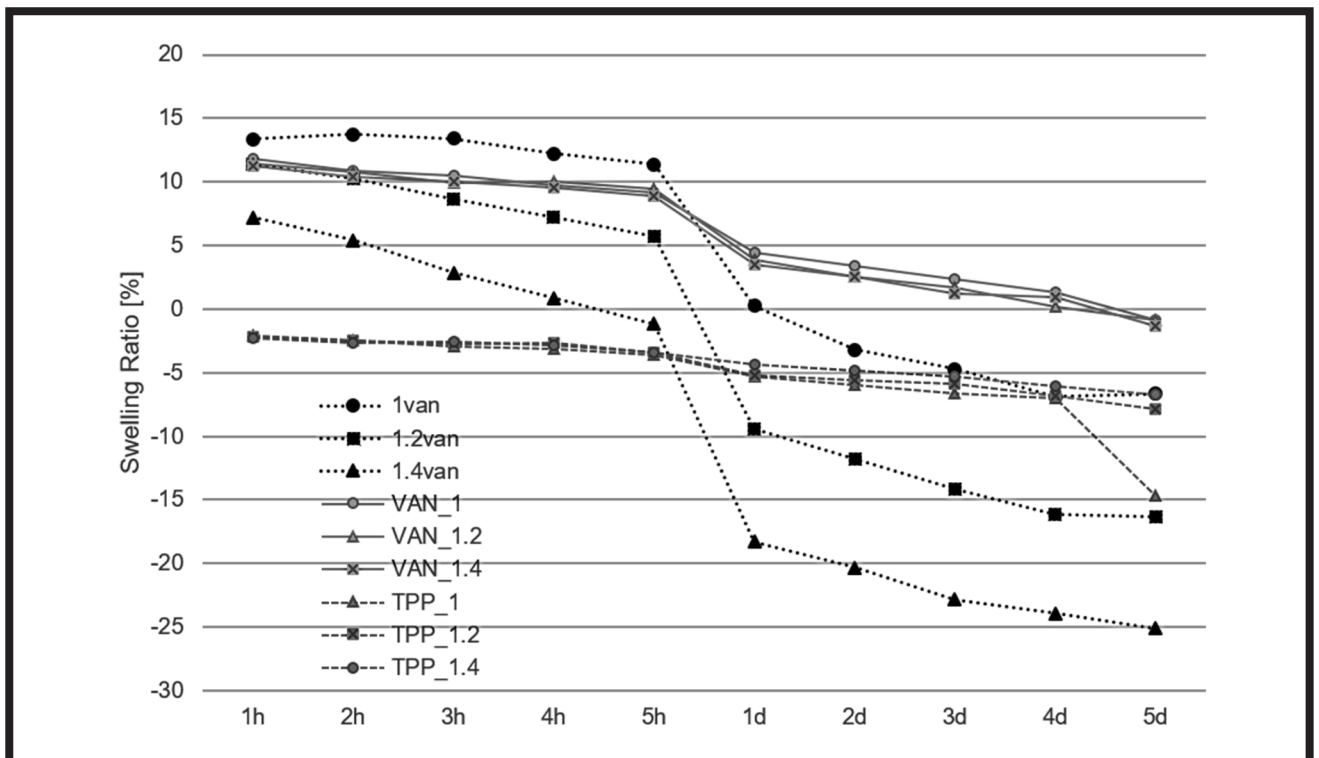


FIG. 6. The swelling ratio results after incubation in PBS solution; single samples were tested for each type of material.

The results of the swelling ratio during incubation in the PBS solution are presented in FIG. 6. The double VAN-crosslinking process had no significant effect on the initial SR in comparison to the single crosslinking – the swelling ratios for these materials were in the range of 7-13%. It was observed how the amount of vanillin added to the polymer solution affected the swelling process. The less vanillin was added, the higher SR was. The more elastic network and the lower amount of linkages facilitated the water absorption by the material. However, swelling of the single crosslinked samples decreased, reaching the negative values after 1 day of incubation. This may suggest the progressive degradation and the release of the non-crosslinked material.

A significant difference was observed for the double crosslinked samples. The TPP-crosslinked samples did not swell and their SR was at a similar level. However, the slow degradation was observed – the obtained values changed during the incubation time from -2.5% to -7.5%. It is important to tailor the swelling character of the hydrogel scaffold for the proper cell migration through the network. Such a match makes it possible to control the transport of the ingredients necessary for tissue regeneration [38]. In addition, the inappropriately high swelling ratio may cause significant changes in the mechanical parameters, such as the chain straightening resulting in the modulus decrease [39].

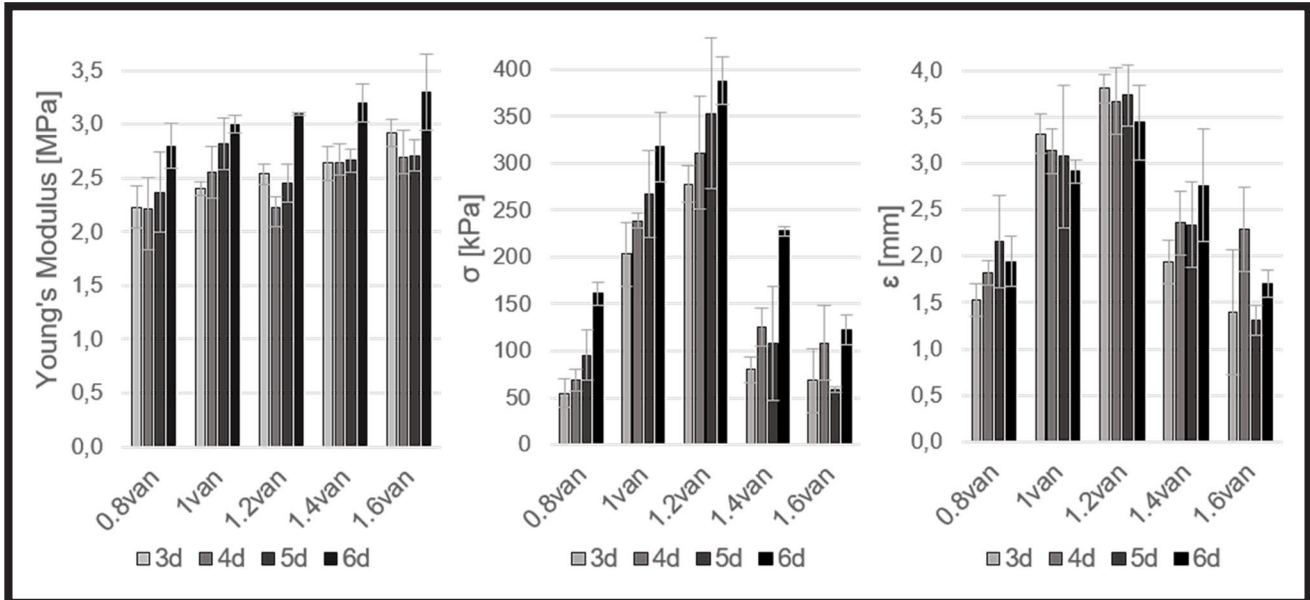


FIG. 7. The results of static compression test for the single crosslinked samples: Young's modulus, compression strength, strain; triplets were tested for each type of material; error bars present standard deviations.

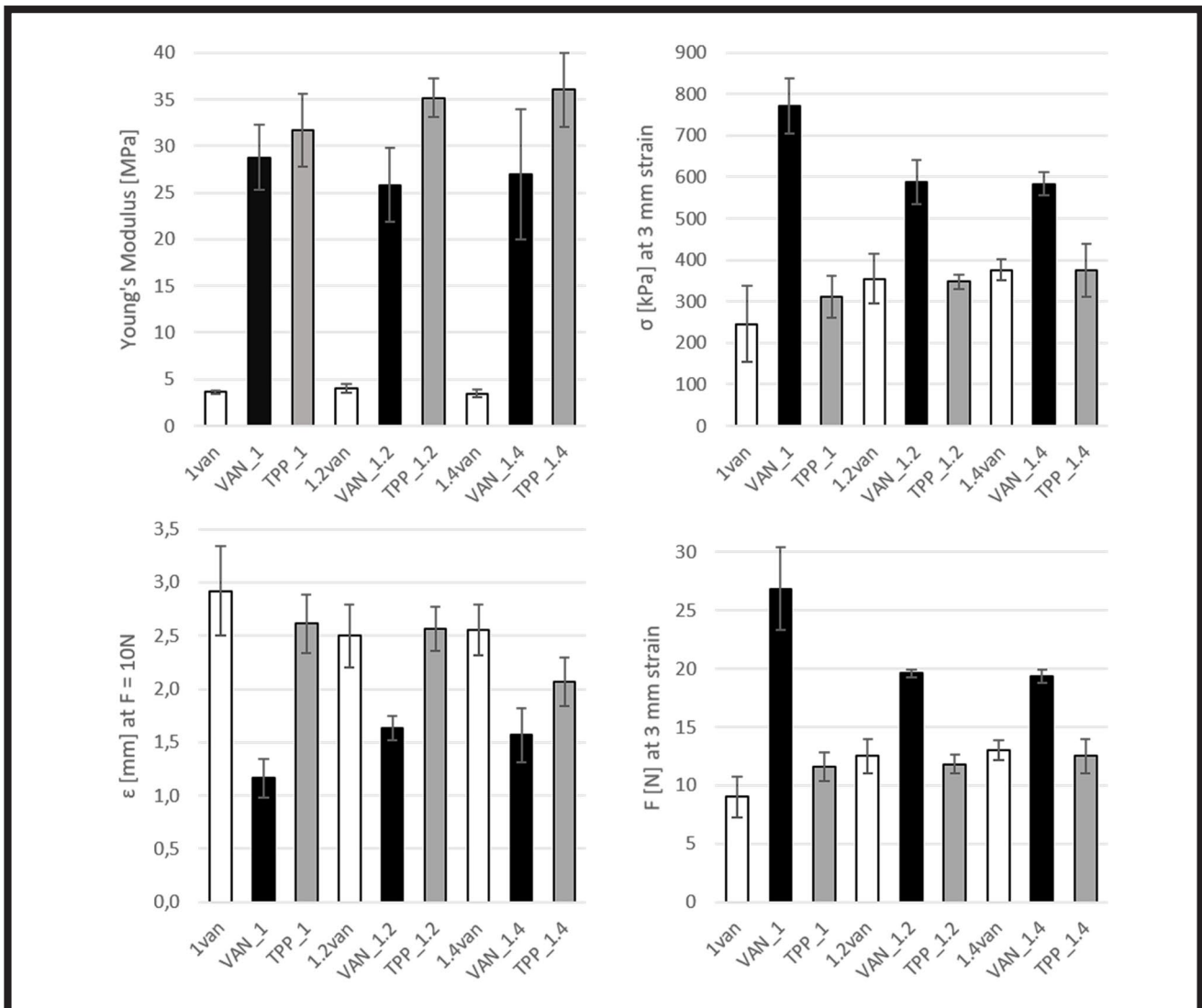


FIG. 8. The results after static compression test for the double crosslinked samples: Young's modulus, compression strength at 3 mm strain, stress at 3 mm strain, strain at stress $F = 10N$; triplets were tested for each type of material; error bars present standard deviations.

The mechanical properties of the single crosslinked samples related to the initial crosslinking time are presented in FIG. 7. The Young's modulus values were similar for all the samples and increased slightly with the crosslinking time, reaching the maximum after the 6th day. However, both the compression strength and the strain values were the highest for the three middle samples, especially for 1.2van. The increase in brittleness for 1.4van and 1.6van resulted in lower compression strength and strain. The residues of unbound vanillin in these materials may have crystallized and acted like an additive making the material less flexible.

The static compression test was also carried out for the double crosslinked samples (FIG. 8). A significant increase in Young's modulus was observed for all the materials after the double crosslinking process, especially for the TPP samples. However, the double VAN samples displayed a more durable structure which resulted in higher compression strength and lower strain, especially for VAN_1.

In comparison to the single crosslinked samples, the double crosslinked ones showed elastic deformation during the compression test. The samples returned to their original shape after the test - in opposite to the single-crosslinked sample, which collapsed at the specific strain.

In general, hydrogels are characterized by poor mechanical properties. However, the hydrogels tested in this work showed efficient properties during compression tests. Both the Young's modulus and the compressive strength reached the values in the range of megapascals – it is very high when compared to the parameters obtained for natural polysaccharide hydrogels in the literature.

Ahearne et al. described alginate and agarose-based hydrogels with the Young's modulus of about 14-15 kPa [40]. Wen et al. proposed chitosan-based hydrogels with high mechanical strength where the values were in the range of 25-200 kPa [41]. The CS-based hydrogels tested in this work exhibited the compression strength with the value of up to 800 kPa. Mirahmadi et al. obtained the chitosan/glycerophosphate/silk fibroin hydrogel with enhanced mechanical properties. DMA test results showed compressive modulus values in the range of 1.5-3.5 kPa [42].

Strong linkages between CS and vanillin provide a significant improvement of mechanical properties after the compression test. Both the Young's modulus and the compressive strength are crucial parameters with regard to tissue regeneration. What is more, mechanical parameters should be adjusted to the repaired tissue. For example, the maximum strength of hyaline cartilage is 1-18 MPa and elastic modulus 0.4-19 MPa [43]. Therefore, the double VAN-crosslinked hydrogels may support the cartilage regeneration due to the appropriate mechanical characteristics.

The compression test results for the double crosslinked samples after 28 days of incubation are shown in FIG. 9. The *in vitro* degradation process of the TPP samples may have weakened the materials. The Young's modulus decrease was of about 80% for the TPP sample, while for the VAN samples it was two-fold lower. Moreover, there was no significant change in the VAN samples' compression strength when comparing this property before and after incubation.

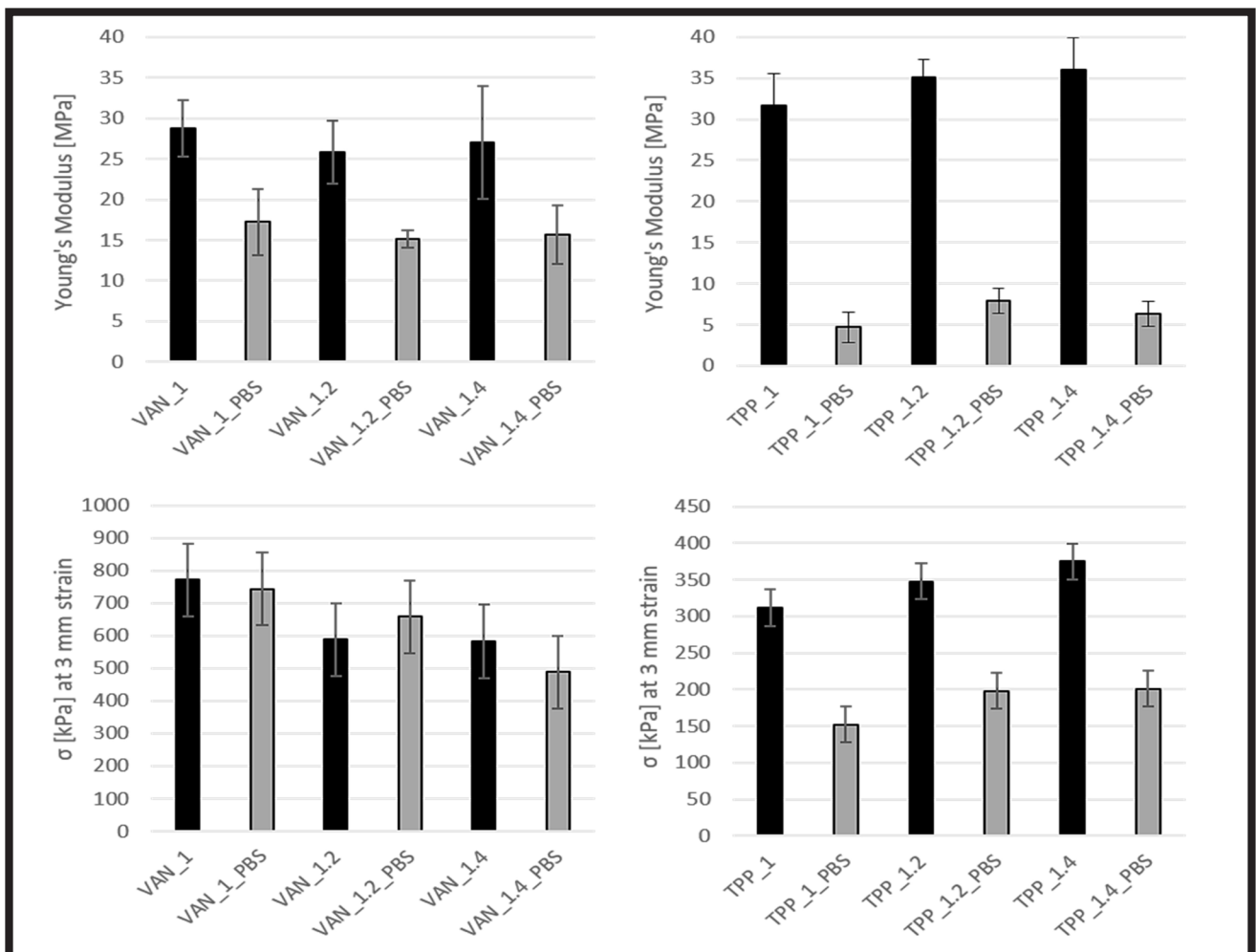


FIG. 9. The results of static compression test for double crosslinked samples before and after 4 weeks incubation in PBS solution; triplets were tested for each type of material; error bars present standard deviations.

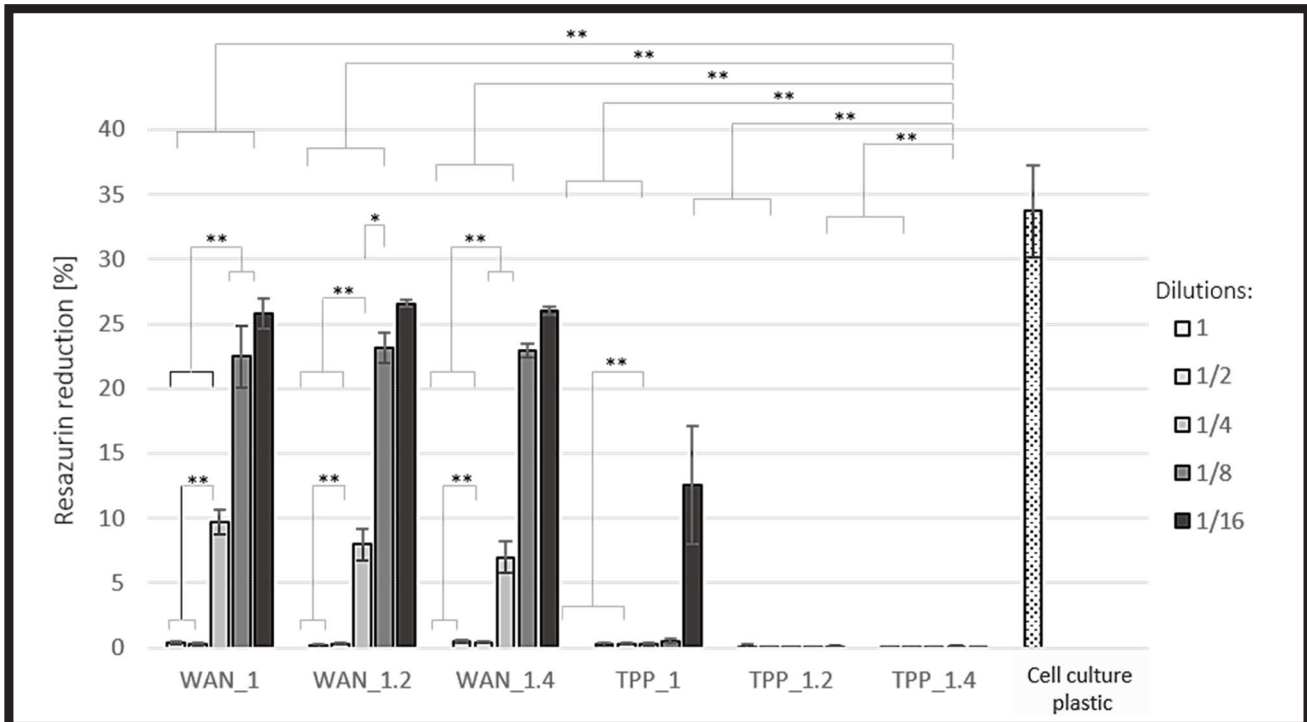


FIG. 10. Metabolic activity of cells cultured for 24 h in the presence of sample extracts in dilutions: 1 (undiluted extract), 1/2, 1/4, 1/8 and 1/16 (statistically significant differences at the level of * $p < 0.05$, ** $p < 0.001$).

The tests proved that all the double VAN-crosslinked samples may constitute beneficial supports for tissue regeneration. As their mechanical properties are stable after 4 weeks of incubation in PBS, the materials may effectively support cell adhesion and proliferation, thus providing the complete sufficient reconstruction of the tissue [44].

FIG. 10 shows the results of the cell metabolic activity (reduction of resazurin) of the cultures incubated for 24 h in the presence of samples extracts at the following dilutions: 1 (undiluted extract), 1/2, 1/4, 1/8 and 1/16. These results were confirmed by the live/dead fluorescent staining test. The representative microscopic images of cells are shown in FIG 11.

The cells incubated in the pure culture medium showed the highest metabolic activity. All the cells visible were alive and retained the correct morphology typical for MG-63 cells (good adhesion, elongated spindle-shape). For all the samples, regardless of the dilution, the cell viability was lower than for the reference sample (pure culture medium). However, at the 1/4 dilution for the double VAN crosslinked samples the live cells were observed. The cells adhesion and proliferation may be limited by the residues of ethanol. The biodegradation results in the PBS solution suggested that a longer pre-incubation period might improve cell viability. Moreover, the higher concentrations of vanillin may reduce the cell viability, e.g. for the 50-200 μM vanillin concentration the lower cell viability was observed. Additionally, the 3-days pre-treatment of incubation in vanillin showed the significantly inhibited effect of the vanillin at the concentration over 5 μM on growth and the spheroid formation of NCI-H460 cells [45]. For all the TPP series samples, only the 1/16 dilution of TPP_1 showed a few live and flattened cells. For the TPP_1.2 and TPP_1.4 the cells revealed no metabolic activity (reduction of resazurin below 0.5%), which indicated the material's cytotoxicity after the double crosslinking with TPP.

Vanillin generally shows a low cytotoxicity effect, however, the crosslinker residues may be potentially toxic and to overcome this disadvantage the lower concentrations should be used. Zou *et al.* discussed the inflammation effect of vanillin and observed the mild inflammation at 4 weeks of the cell culture [46]. A similar effect was described for TPP by Gurses *et al.* With an increasing amount of sodium triphosphate and sodium citrate, the significantly decreased human kidney cell viability was noticed [47]. Freitas Mariano *et al.* also described a negative influence of the TPP addition in the CS matrix on cell viability [48]. Therefore, it is necessary to determine the sufficient concentration of a crosslinking agent to reduce the cytotoxic effect of the hydrogel.

Conclusions

The double crosslinked chitosan hydrogels with the improved mechanical properties and chemical stability were obtained in this study with the use of vanillin as a natural crosslinking agent. The efficient mechanical properties and higher chemical stability prove high effectiveness of the double crosslinking process using vanillin. The results of the *in vitro* biological test revealed cytotoxicity of the double TPP crosslinked material. Although the polymer and the crosslinking agent used in the study are biocompatible, even a small amount of the solvent – ethanol – may be a barrier for cell proliferation. However, the cell viability could be improved, e.g. by a longer incubation time (to wash out the residues of cytotoxic solvents). Determining the sufficient concentration of the crosslinking agent should also be considered as an important aspect. Further studies are required to improve cytocompatibility of the testes hydrogels.

In the next step, the double VAN crosslinked hydrogels will be modified with additives, such as hydroxyapatite or graphene oxide to evaluate their influence on the material properties. Then, the choice of appropriate layers and optimization of the technology may result in mechanically stronger hierarchical structures dedicated for bone and cartilage tissue engineering.

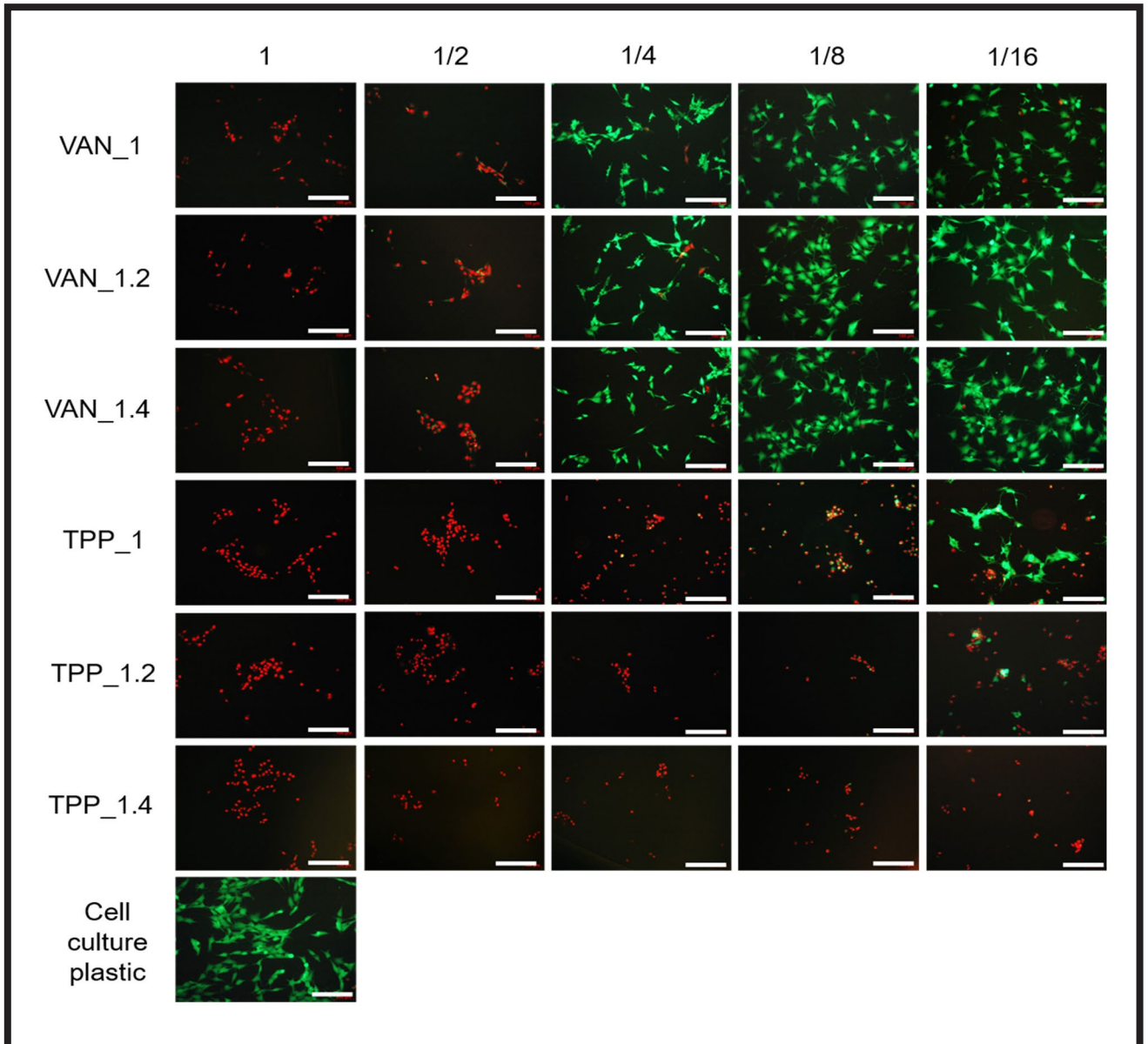


FIG. 11. Live/dead staining of cells cultured for 24 h in the presence of sample extracts in dilutions: 1 (undiluted), 1/2, 1/4, 1/8 and 1/16 (scale bar: 200 μ m).

Acknowledgments

This study was funded by The National Centre for Research and Development (NCBR) in the program STRATEGMED III (project no. STRATEGMED3/303570/7/NCBR/2017).

ORCID iDs

M. Hunger:

<https://orcid.org/0000-0002-9854-166X>

P. Domalik-Pyzik:

<https://orcid.org/0000-0002-5978-5688>

K. Reczyńska:

<https://orcid.org/0000-0002-5266-9131>

J. Chłopek:

<https://orcid.org/0000-0003-3293-9082>

References

- [1] Croisier F., Jérôme C.: Chitosan-based biomaterials for tissue engineering. *European Polymer Journal* 49 (2013) 780–792.
- [2] Koosha M., Raoufi M., Moravvej H.: One-pot reactive electrospinning of chitosan/PVA hydrogel nanofibers reinforced by halloysite nanotubes with enhanced fibroblast cell attachment for skin tissue regeneration. *Colloids Surfaces B Biointerfaces* 179 (2019) 270–279.
- [3] Huang L. *et al.*: Antibacterial poly (ethylene glycol) diacrylate/chitosan hydrogels enhance mechanical adhesiveness and promote skin regeneration. *Carbohydrate Polymers* 225 (2019) 115110.
- [4] Moreira C.D.F., Carvalho S.M., Sousa R.G., Mansur H.S., Pereira M.M.: Nanostructured chitosan/gelatin/bioactive glass in situ forming hydrogel composites as a potential injectable matrix for bone tissue engineering. *Materials Chemistry and Physics* 218 (2018) 304–316.
- [5] Saekhor K. *et al.*: Preparation of an injectable modified chitosan-based hydrogel approaching for bone tissue engineering. *International Journal of Biological Macromolecules* 123 (2019) 167–173.
- [6] Liu J., Yang B., Li M., Li J., Wan Y.: Enhanced dual network hydrogels consisting of thiolated chitosan and silk fibroin for cartilage tissue engineering. *Carbohydrate Polymers* 227 (2020) 115335.
- [7] Shao J., Ding Z., Li L., Chen Y., Zhu J., Qian Q.: Improved accumulation of TGF- β by photopolymerized chitosan/silk protein bio-hydrogel matrix to improve differentiations of mesenchymal stem cells in articular cartilage tissue regeneration. *Journal of Photochemistry and Photobiology B: Biology* 203 (2020) 111744.
- [8] Jafarkhani M., Salehi Z., Nematian T.: Preparation and characterization of chitosan/graphene oxide composite hydrogels for nerve tissue Engineering. *Materials Today: Proceedings* 5 (2018) 15620–15628.
- [9] Badhe R. V. *et al.*: A composite chitosan-gelatin bi-layered, biomimetic macroporous scaffold for blood vessel tissue engineering. *Carbohydrate Polymers* 157 (2017) 1215–1225.
- [10] Ravishankar K., Dhamodharan R.: Advances in chitosan-based hydrogels: Evolution from covalently crosslinked systems to ionotropically crosslinked superabsorbents. *Reactive and Functional Polymers* 149 (2020) 104517.
- [11] Mikhailov S. N. *et al.*: Crosslinking of Chitosan with Dialdehyde Derivatives of Nucleosides and Nucleotides. Mechanism and Comparison with Glutaraldehyde. *Nucleosides, Nucleotides and Nucleic Acids* 35 (2016) 114–129.
- [12] Zhang Z.H. *et al.*: Enhancing mechanical properties of chitosan films via modification with vanillin. *International Journal of Biological Macromolecules* 81 (2015) 638–643.
- [13] Stroescu M. *et al.*: Chitosan-vanillin composites with antimicrobial properties. *Food Hydrocolloids* 48 (2015) 62–71.
- [14] Tomadoni B., Ponce A., Pereda M., Ansorena M.R.: Vanillin as a natural cross-linking agent in chitosan-based films: Optimizing formulation by response surface methodology. *Polymer Testing* 78 (2019) 105935.
- [15] Cestari A.R., Vieira E.F.S., Mattos C.R.S.: Thermodynamics of the Cu(II) adsorption on thin vanillin-modified chitosan membranes. *The Journal of Chemical Thermodynamics* 38 (2006) 1092–1099.
- [16] Zou Q., Li J., Li Y.: Preparation and characterization of vanillin-crosslinked chitosan therapeutic bioactive microcarriers. *International Journal of Biological Macromolecules* 79 (2015) 736–747.
- [17] Walke S. *et al.*: Fabrication of chitosan microspheres using vanillin/TPP dual crosslinkers for protein antigens encapsulation. *Carbohydrate Polymers* 128 (2015) 188–198.
- [18] Berger J. *et al.*: Structure and interactions in covalently and ionically crosslinked chitosan hydrogels for biomedical applications. *European Journal of Pharmaceutics and Biopharmaceutics* 57 (2004) 19–34.
- [19] Guaresti O. *et al.*: Synthesis and characterization of a biocompatible chitosan-based hydrogel cross-linked via 'click' chemistry for controlled drug release. *International Journal of Biological Macromolecules* 102 (2017) 1–9.
- [20] Gohil S.V. *et al.*: Evaluation of enzymatically crosslinked injectable glycol chitosan hydrogel. *Journal of Materials Chemistry B* 3 (2015) 5511–5522.
- [21] Sun Z., *et al.*: Multistimuli-Responsive, Moldable Supramolecular Hydrogels Cross-Linked by Ultrafast Complexation of Metal Ions and Biopolymers. *Angewandte Chemie International Edition* 54 (2015) 7944–7948.
- [22] Takei T. *et al.*: Autoclavable physically-crosslinked chitosan cryogel as a wound dressing. *Journal of Bioscience and Bioengineering* 125 (2018) 490–495.
- [23] Smith R. A., Walker R. C., Levit S. L., Tang C.: Single-step self-assembly and physical crosslinking of PEGylated chitosan nanoparticles by tannic acid. *Polymers (Basel)* 11 (2019) 749.
- [24] Sacco P. *et al.*: Insight into the ionotropic gelation of chitosan using tripolyphosphate and pyrophosphate as cross-linkers. *International Journal of Biological Macromolecules* 92 (2016) 476–483.
- [25] Csaba N. *et al.*: Ionically crosslinked chitosan/tripolyphosphate nanoparticles for oligonucleotide and plasmid DNA delivery. *International Journal of Pharmaceutics* 382 (2009) 205–214.
- [26] Czechowska-Biskup R. *et al.*: Determination of degree of deacetylation of chitosan - Comparison of methods. *Progress on Chemistry and Application of Chitin and its Derivatives* 17 (2012) 5–20.
- [27] Kosheleva R., *et al.*: Effect of grafting on chitosan adsorbents. *Composite Nanoadsorbents*, Elsevier, Oxford, U.K., 2018, 49–66.
- [28] Aizat M. A., Aziz F.: 12 - Chitosan Nanocomposite Application in Wastewater Treatments. *Nanotechnology in Water and Wastewater Treatment: Theory and Applications*, Elsevier, 2018, 243–265.
- [29] Lv S. H.: High-performance superplasticizer based on chitosan, in *Biopolymers and Biotech Admixtures for Eco-Efficient Construction Materials*, Elsevier Inc., 2016, 131–150.
- [30] Xu C., Zhan W., Tang X., Mo F., Fu L., Lin B.: Self-healing chitosan/vanillin hydrogels based on Schiff-base bond/hydrogen bond hybrid linkages. *Polymer Testing* 66 (2018) 155–163.
- [31] Ozbolat I. T.: The Bioink**With contributions by Monika Hopsodiuk and Madhuri Dey, The Pennsylvania State University, 3D Bioprinting, Elsevier, 2017, 41–92.
- [32] Józwiak T. *et al.*: Effect of ionic and covalent crosslinking agents on properties of chitosan beads and sorption effectiveness of Reactive Black 5 dye. *Reactive and Functional Polymers* 114 (2017) 58–74.
- [33] Hourant P.: General Properties of the Alkaline Phosphates: - Major Food and Technical Applications, *Phosphorus Research Bulletin* 15 (2004) 85–94.
- [34] Singh S.: Effects of different pH and oxygen levels on proliferation and chondrogenic differentiation of human mesenchymal stem cells cultured in hydrogels, MSc thesis, Department of Applied Physics, Chalmers University of Technology, Gothenburg, Sweden 2014
- [35] Galow A.M. *et al.*: Increased osteoblast viability at alkaline pH in vitro provides a new perspective on bone regeneration. *Biochemistry and Biophysics Reports* 10 (2017) 17–25.
- [36] Noeaid P., Salih V., Beier J. P., Boccaccini A. R.: Osteochondral tissue engineering: Scaffolds, stem cells and applications. *Journal of Cellular and Molecular Medicine* 16 (2012) 2247–2270, 2012.
- [37] Xiao H. *et al.*: Osteochondral repair using scaffolds with gradient pore sizes constructed with silk fibroin, chitosan, and nano-hydroxyapatite. *International Journal of Nanomedicine* 14 (2019) 2011–2027.
- [38] Zhu J., Marchant R.E.: Design properties of hydrogel tissue-engineering scaffolds, *Expert Review of Medical Devices* 8 (2011) 607–626.
- [39] Young S.A. *et al.*: In situ-forming, mechanically resilient hydrogels for cell delivery. *Journal of Materials Chemistry B* 7 (2019) 5742–5761.
- [40] Ahearne M. *et al.*: Mechanical Characterisation of Hydrogels for Tissue Engineering Applications *Hydrogels for Tissue Engineering*, 2008.
- [41] Wen Y., Li F., Li C., Yin Y., Li J.: High mechanical strength chitosan-based hydrogels cross-linked with poly(ethylene glycol)/polycaprolactone micelles for the controlled release of drugs/growth factors. *Journal of Materials Chemistry B* 5 (2017) 961–971.
- [42] Mirahmadi F. *et al.*: Enhanced mechanical properties of thermosensitive chitosan hydrogel by silk fibers for cartilage tissue engineering. *Materials Science and Engineering: C* 33 (2013) 4786–4794.
- [43] Silver F.H. *et al.*: *Mechanical Properties of Tissues*, Biomaterials Science and Biocompatibility, Springer New York, 1999, 187–212.
- [44] Ansari S. *et al.*: Engineering of gradient osteochondral tissue: From nature to lab. *Acta Biomaterialia* 87 (2019) 41–54.
- [45] Srinual S. *et al.*: Suppression of cancer stem-like phenotypes in NCI-H460 lung cancer cells by vanillin through an Akt-dependent pathway. *International Journal of Oncology* 50 (2017) 1341–1351.
- [46] Zou Q., Li J., Li Y.: Preparation and characterization of vanillin-crosslinked chitosan therapeutic bioactive microcarriers. *International Journal of Biological Macromolecules* 79 (2015) 736–747.
- [47] Gurses M. S., Erkey C., Kizilil S., Uzun A.: Characterization of sodium tripolyphosphate and sodium citrate dehydrate residues on surfaces. *Talanta* 176 (2018) 8–16.
- [48] Freitas Mariano K.C. *et al.*: Influence of chitosan-tripolyphosphate nanoparticles on thermosensitive polymeric hydrogels: structural organization, drug release mechanisms and cytotoxicity. *International Journal of Polymeric Materials and Polymeric Biomaterials* 69 (2020) 592–603.

PREPARATION AND CHARACTERIZATION OF BIO-HYBRID HYDROGEL MATERIALS

DAGMARA MALINA^{1*} , EWELINA KRÓLICKA² ,
KATARZYNA BIALIK-WĄS² , KLAUDIA PLUTA¹ 

¹ INSTITUTE OF INORGANIC CHEMISTRY AND TECHNOLOGY

² INSTITUTE OF ORGANIC CHEMISTRY AND TECHNOLOGY
CRACOW UNIVERSITY OF TECHNOLOGY

24 WARSZAWSKA ST., 31-155 CRACOW, POLAND

*E-MAIL: DAGMARA.MALINA@PK.EDU.PL

Abstract

In recent decades, research has focused on the development of modern hydrogel dressings due to their open porous structure, moisture retention and good mechanical strength, which ensures an optimal environment for cell migration and proliferation. Active hydrogel dressings, currently available on the market, are not endowed with additional medicinal substances. In this work the authors attempted to introduce a carrier-drug system into the hydrogel matrix to improve the wound healing process and the tissue recovery. The main goal of the research was to obtain the bio-hybrid sodium alginate/poly(vinyl alcohol)/Aloe vera (SA/PVA/AV)-based hydrogel matrices modified with the thermosensitive polymeric carrier – the active substance (hydrocortisone) system. First, thermosensitive polymeric nanocarriers were obtained, then the encapsulation was conducted, using varied amounts of hydrocortisone (25 and 50 mg) to maintain the stability of the resulting emulsions. The last stage was preparing the bio-hybrid hydrogel matrices by the chemical cross-linking method. The non-invasive dynamic light scattering (DLS) technique was employed for the analysis of the average particle size of the polymeric carriers and the carrier-drug systems. Moreover, the studies also determined the swelling behaviour and the gel fraction of the obtained bio-hybrid hydrogel matrices modified with carrier-drug systems by the infrared spectroscopy (FT-IR). The presented research results constitute a good experimental basis for further modifications, the final effect of which is assumed to be a modern bio-hybrid 3rd generation dressing.

Keywords: hydrogel matrix, drug delivery system, carrier-drug system, synthesis, hydrocortisone

[*Engineering of Biomaterials* 155 (2020) 12-16]

doi:10.34821/eng.biomat.155.2020.12-16

Introduction

Hydrogels are one of the most promising materials widely used in medicine, due to the ability to control the water content and sensitivity to stimulus changes (e.g. temperature and pH). They are characterized by properties similar to biological tissues and they exhibit high biocompatibility [1,2]. Besides, various substances can be incorporated into the hydrogel matrix to induce a change in the initial physico-chemical properties of the material. In the world literature here are many reports on hybrid hydrogel matrices modified with active substances or drugs [2-4].

In the pharmaceutical and medicine industries, hydrogels are used primarily in the production of active dressings, in tissue engineering and as systems for the controlled delivery of active substances [1,4-6]. In terms of the controlled and prolonged release of active substances, polymer nanoparticles enable effective penetration of active substances, proteins or DNA through cell membranes. They also demonstrate stability in the blood and they do not stimulate the immune system and inflammatory processes. The most commonly obtained structures exhibit nanometric sizes (range 100-500 nm). Polymer nanoparticles are stable, they have colloidal structures and exist in the form of nanospheres and nanocapsules. The materials used in nanopharmacology are mainly biodegradable polymers, e.g. chitosan, polylactic acid, gelatin, (N-(2-hydroxypropyl) methacrylamide) and their copolymers [7-9].

The pharmaceutical market offers a wide range of dermatological preparations, as even the smallest skin lesions may be associated with an allergic reaction or a serious disease. Patients use various types of ointments, gels or lotions containing active substances, such as salicylic acid, hydrocortisone and plant extracts. Ideally, a skin substitute scaffold should maintain the moist healing environment on the wound surface. It should also persist long enough so that the cells have enough time to migrate through the scaffold and build a new extracellular matrix responsible for the movement of keratinocytes and growth factors. Thus, the wound starts to be covered with a single epithelial layer. Therefore, the hydrogels properties, such as the ability to create a permanent moist medium in the wound and to absorb wound exudates, are a key factor to maintain cellular activity by means of the substances promoting the skin reconstruction [10-12].

A bio-hybrid hydrogel material well described in the literature is a hydrogel based on hydroxyl chitin enriched with tannic acid used to treat skin ulcers and burns. The hydrogel is endowed with strong antioxidant, antibacterial and hemostatic properties. Metal ions which are chelating sites with multiple galloyl groups of tannic acid form a stable complex [13,14]. Hybrid hydrogel matrices based on poly(vinyl alcohol), chitosan and silver nanoparticles are widely used in medicine due to the antibacterial properties of nanometric silver against many bacterial and fungal strains [15,16]. Also, in cancer therapies, a promising material is the chitosan/nanogold hybrid hydrogel used as a delivery system for drugs, e.g. doxorubicin (DOX). Studies have shown that the drug released from the hydrogel is biologically active but has lower cytotoxicity due to the controlled release in the expected location in the patient's body, such an approach is called targeted therapy [17].

In dermatology, the transdermal drug delivery of the hydrophobic active substances, such as: hydrocortisone, fluocinolone acetonide, tazarotene, is an ongoing challenge. Hydrocortisone is a glucocorticoid steroid hormone commonly used in the topical treatment of dermatological diseases, such as: atopic dermatitis, psoriasis, mycosis and acne. In general, this active substance is characterized by anti-inflammatory and anti-allergic activities [18], it can be used also for adrenal replacement therapy. However, as hydrocortisone is highly hydrophobic, it is difficult to synthesize it and later – to develop its efficient application procedures. Therefore, it seems beneficial to combine hydrocortisone with a hydrogel matrix used as a carrier. The studies so far have indicated that hydrocortisone may be incorporated into hydrogels based on chitosan, gelatin, methylcellulose or carboxymethylcellulose [19,20], which allows to obtain better therapeutic effects within the significantly shortened treatment time.

The main objective of the research presented in this paper was to prepare the bio-hybrid SA/PVA/AV based hydrogel matrices modified with the thermosensitive polymeric carrier and to characterize the active substance (hydrocortisone) system in terms of the basic physicochemical and structural properties.

Materials and Methods

N-isopropylacrylamide, N, N'-methylene bisacrylamide (NMBA), hydrocortisone, sodium alginate and poly(ethylene glycol) diacrylate (PEGDA) $M_n = 700$ g/mol (used as a cross-linking agent) were purchased from Sigma – Aldrich (Germany). Poly(vinyl alcohol) ($M_n = 72\,000$ g/mol), ammonium persulphate employed as an initiator and glycerine were acquired from POCH SA (Poland). *Aloe vera* lyophilisate was purchased from a shop with cosmetics and herbal raw materials - Zrob sobie krem, Poland. All the applied chemical reagents were of high purity.

The first research stage consisted in the synthesis of thermosensitive polymeric carriers with the radical polymerization reaction, using N-isopropylacrylamide, N, N'-methylene bisacrylamide and ammonium persulfate, according to the literature data with some modifications [21]. After that, the active substance (hydrocortisone) was introduced into the polymeric carriers - the drug amount was 25 or 50 mg – based on the commercially available ointments. The emulsion mixing was performed for 10 min, 3 h, 5 h and 24 h. The obtained samples were analyzed using the dynamic light scattering (DLS) technique and afterwards they were lyophilized prior to being introduced into the hydrogel structure. In the last stage the bio-hybrid hydrogel matrices were synthesized via the chemical cross-linking method developed in the authors' previously published research which is currently the subject of a patent application [22]. In order to obtain the SA/PVA/AV hydrogels, the following solutions were prepared: a 5% solution of poly(vinyl alcohol), 2% solution of sodium alginate, 2% solution of *Aloe vera* extract and 1% solution of ammonium persulfate. Next, the proper amounts of the polymers solutions in the ratio 1:1 and the constant amounts of poly(ethylene glycol) diacrylate (7.5%) and glycerin (1.7%) were mixed. A slight addition of glycerin ensured transparency of the material and had a positive effect on the membrane flexibility. Subsequently, the mixtures were heated to 70°C and the 4.4% (v/v) ammonium persulfate was added. After that, all the specimens were poured into Petri dishes and placed on a heating plate with a temperature of 80°C for 1.5 h.

The non-invasive dynamic light scattering (DLS) technique was used to analyze the average particle size of the polymer carriers and the carrier-drug systems. The conducted research also included determining the swelling behaviour and the gel fraction. It also determined the chemical structure of the resultant bio-hybrid hydrogel matrices modified with carrier-drug systems via the infrared spectroscopy (FT-IR).

The average particle size measurements were performed using Zetasizer Nano ZS device produced by Malvern Instruments Ltd., which allows to assess the particle sizes in the range from 0.6 to 6000 nm. Each sample was measured three times, with each measurement consisting of several runs in order to determine the mean values precisely. The measurements were carried out at 25°C.

The swelling behaviour (absorption capacity) ratio was evaluated by immersing the samples in the isotonic buffer used in biological application (PBS, phosphate-buffered saline, pH = 7.4) and the distilled water at 37°C.

The dried and weighted (W_d) hydrogel samples were soaked in the immersion fluids. The swollen samples were taken out and weighted (W_s) after 1 and 24 h. The water uptake of all tested hydrogel samples was determined using the following equation: absorption capacity [g/g] = $(W_d - W_s)/W_d$.

In order to determine the gel fraction (GF%), the obtained hydrogel materials were cut into 10 x 10 mm pieces, dried at 40°C for 24 h and weighted (W_0). Then dried hydrogel samples were soaked in the distilled water for 48 h up to an equilibrium swelling weight to remove the leachable or soluble parts from the matrices. Then, the gel materials were dried again in the same conditions and weighted (W_e). The gel fraction (GF%) was calculated by the following equation:

$$\%GF = W_e/W_0 \cdot 100\%$$

To identify the chemical structure of the hydrogels, the infrared spectroscopy was used with Thermo Scientific Nicolet iS5 FTIR spectrometer equipped with iD7 ATR accessory in the range of 4000 - 400 cm^{-1} .

Results and Discussions

The size of the drug carriers is an extremely important parameter. Therefore, in this study, the key analysis consisted in determining the average particle size of the thermosensitive polymeric carrier and the carrier - drug system. The average size of the unloaded (empty) polymeric carriers particles was 118 nm, but having removed the unreacted monomer via the dialysis method, this parameter decreased below 100 nm. In turn, the encapsulated carriers analysis showed that the presence of the drug increased the particle size. Additionally, the drug amount and the encapsulation time directly affected the average particle size, which is shown in TABLE 1.

TABLE 1. The average particle size of polymeric carrier - drug systems.

System number	Drug amount	Mixing time	Average particle size
1	25 mg	10 min	400 nm
2		3 h	391 nm
3		5 h	505 nm
4		24 h	1150 nm
5	50 mg	10 min	425 nm
6		3 h	617 nm
7		5 h	1049 nm
8		24 h	2285 nm

Comparing the systems containing the same drug amount but with the different mixing time, it can be concluded that the system prolonged mixing caused a significant increase in the particle size. The systems with the highest amount of drug displayed a much larger average particle size after the 24-hour mixing (2285 nm) than after the 3-hour mixing (617 nm). However, it was possible to obtain stable systems without the agglomeration effect with the average size below 500 nm. These thermosensitive carriers – the hydrocortisone systems were used for further research on developing the bio-hybrid hydrogel materials. FIG. 1 presents the photos of the obtained various systems.

The swelling tests results revealed that the obtained bio-hybrid hydrogel matrices had a slightly higher absorption capacity in the water environment than in the phosphate buffer (FIG. 2).

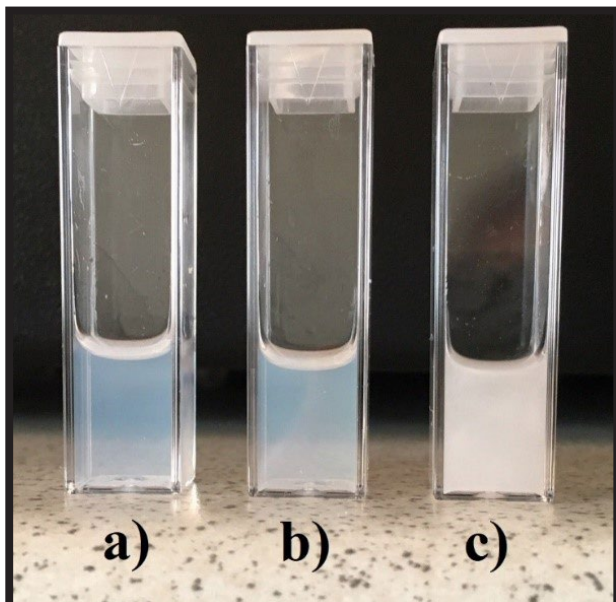


FIG. 1. Photos of the thermosensitive polymeric carrier – the hydrocortisone systems obtained after mixing for: a) 10 min, b) 3 h and c) 24 h.

The obtained results were very similar, however, the samples containing a higher drug concentration revealed a slightly higher swelling degree in each of the used media. This phenomenon resulted from the fact that the packing density of the chains in the hydrogel matrix decreased with adding new components to the system. When a higher concentration of the drug was released from the hydrogel matrix, additional gaps replacing the absorbed fluid were created. It was observed that the swelling degree decreased with time, probably due to the lack of free hydroxyl groups and/or spherical hindrance. As a result, no further hydration occurred. Based on the results, the tested bio-hybrid hydrogel matrices proved to be stable materials that did not change the shape during the incubation (they only slightly increased in size). Comparing the media used in the study, the samples in the PBS fluid showed the better stability and the more compact and flexible structure than the samples incubated in the distilled water.

The gel fraction value (%GF) represents the insoluble gel fraction as a result of inter-molecules crosslinking formation. The obtained bio-hybrid hydrogel matrices with the carrier-drug system were characterized by higher levels of crosslinking (over 67%) (FIG. 3). The content of the gel fraction reached the value of 66-67%, while the addition of the drug slightly increased this parameter. Also, the most important fact is that the thermosensitive polymer carrier - hydrocortisone did not reduce the degree of matrix crosslinking and it was even slightly higher. Moreover, with the cross-linking increase, the mechanical properties of the hydrogel increased too and thus the mechanical resistance of the material.

The chemical structure of the thermosensitive carrier – hydrocortisone systems and the bio-hybrid hydrogel matrices are presented in FIG. 4 and 5, respectively.

In the case of the modified thermosensitive carrier – drug system (FIG. 5), a much more intense band was observed in the range of 3500-3000 cm^{-1} which originated from the stretching vibrations of the O-H group the N-H group vibrations and most likely - from the strong hydrogen interactions that occurred between individual components.

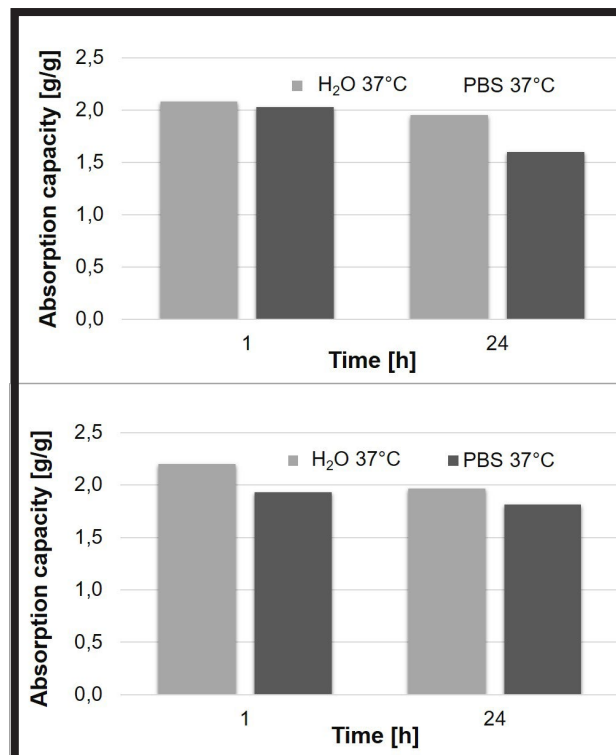


FIG. 2. The absorption capacity of the bio-hybrid hydrogel matrix modified with the thermosensitive polymeric carrier - hydrocortisone at varied drug concentrations in different fluids: a) 25 mg of the drug, b) 50 mg of the drug.

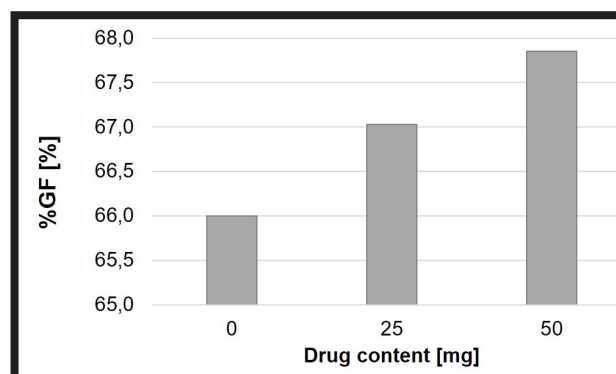


FIG. 3. The gel fraction of hydrogel material and bio-hybrid hydrogel matrices modified with the thermosensitive polymeric carrier - hydrocortisone at varied drug concentrations.

This was also confirmed by the determined %GF which was the highest for the bio-hybrid matrices containing the thermosensitive carrier – drug system, thus indicating a significant matrix cross-linking. Moreover, this broadest band in the range 3500-3000 cm^{-1} corresponded to the O-H groups stretching vibrations coming from SA, PVA and *Aloe vera*. Later, at a wavenumber of 2940 cm^{-1} the characteristic band appeared, which can be assigned to the C-H group stretching vibrations. The band at 1350-1330 cm^{-1} could be attributed to the bending vibrations of C-H and O-H. Additionally, all the FT-IR spectra showed a marked vibration band centered at 1730 cm^{-1} - exhibiting the presence of an ester group characteristic of poly(ethylene glycol) diacrylate (PEGDA). The absorption peaks of PEGDA were also seen at 1164, 1190, 1035 cm^{-1} for the C-O-C stretching [23].

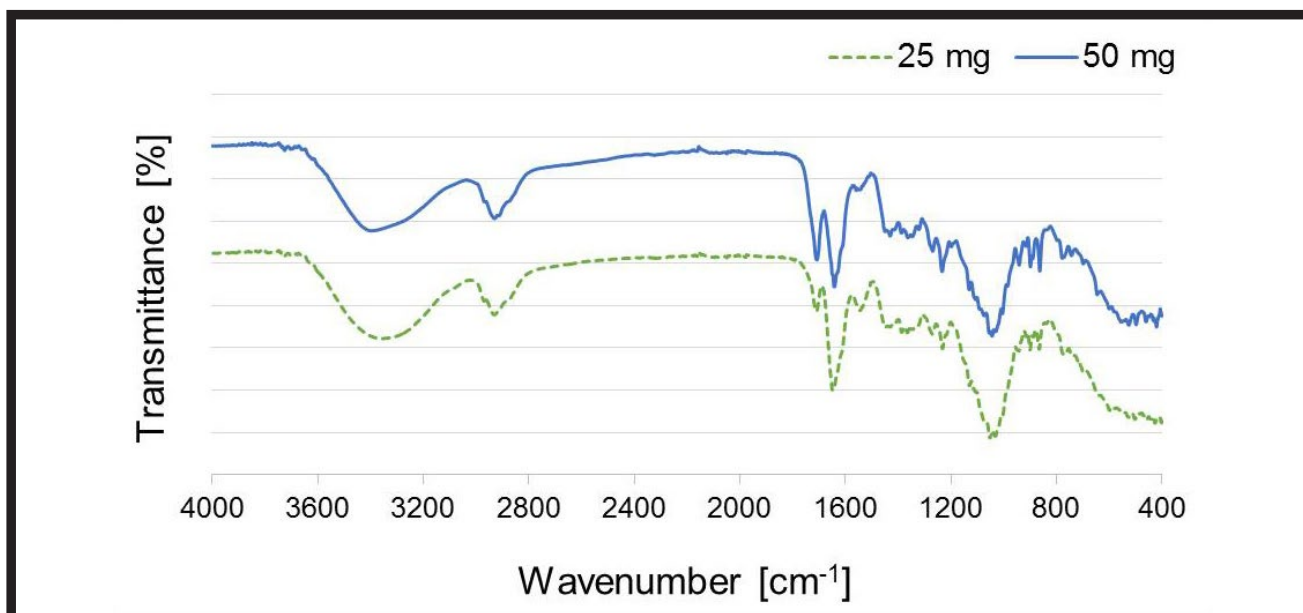


FIG. 4. The FT-IR spectra of thermosensitive polymeric carrier - hydrocortisone at varied drug concentrations.

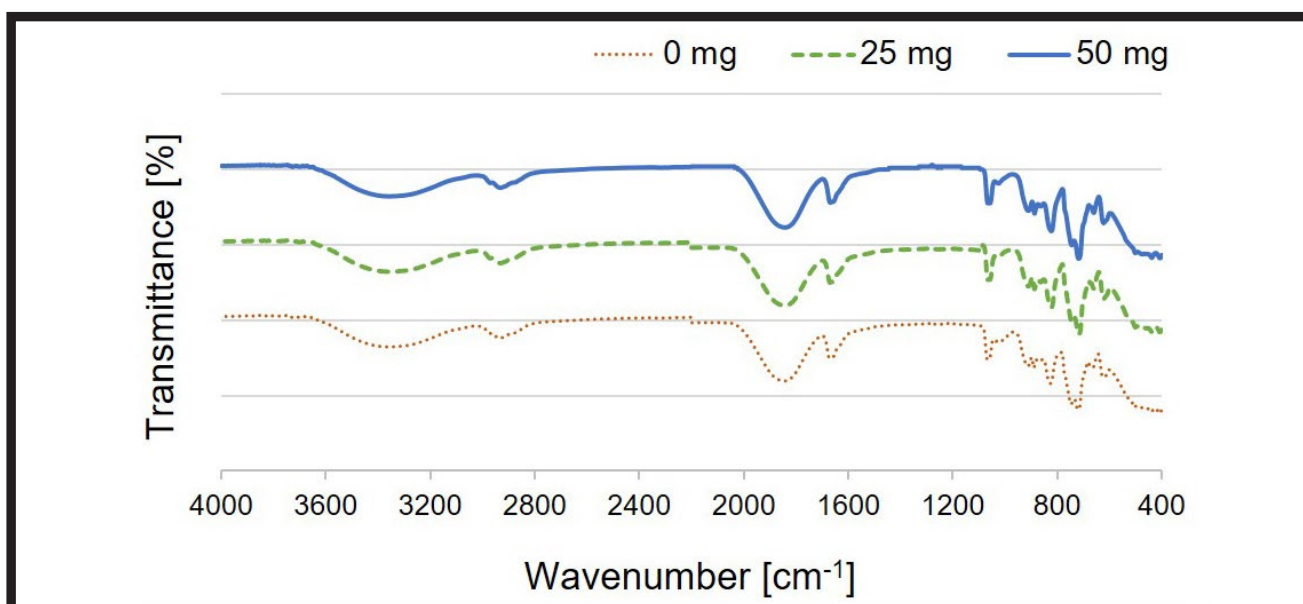


FIG. 5. The FT-IR spectra of the bio-hybrid hydrogel material modified with the thermosensitive polymeric carrier - hydrocortisone at varied drug concentrations.

In the case of the sample with 50 mg hydrocortisone (FIG. 4), there was a significantly more intense absorption band in the range of 1870-1600 cm⁻¹, coming from the C=O stretching vibrations of the drug structure. The presence of the intense absorption band in the range of 1150-1100 cm⁻¹ proved the valence vibrations from the C-N group in the systems. This was confirmed by the presence of N-H and C-N groups of poly(N-isopropylacrylamide). However, the peaks at 1607 and 1450 cm⁻¹ corresponded to the asymmetric and symmetric stretching vibrations of carboxylate anion (COO⁻), respectively. Moreover, there were bands located at 985 and 810 cm⁻¹ assigned to the COH out-of-plane bending and -CH₂ twisting [24-25].

The characteristic absorption bands for the -C-H (3000-2850 cm⁻¹), -C-C (1452-1402 cm⁻¹) and -C-O (1200-1000 cm⁻¹) groups were also evident both in the bio-hybrid hydrogel materials and in the thermosensitive carrier - hydrocortisone and probably they overlapped [23,26].

Conclusions

The application of thermosensitive polymers as drug carriers may increase the therapeutic value of the drugs used by modifying their solubility, retention time and crossing biological barriers. This contributes to the reduction of side effects that result from the prolonged use of the medicament and higher effectiveness of the therapy.

The analysis of the encapsulated polymeric carriers showed that the presence of the drug, its amount and the encapsulation time increased the average size of particles. It was possible to obtain the time-stable empty thermosensitive carrier with the average particle size below 100 nm and the encapsulated system - containing hydrocortisone introduced into hydrogel structure - with the average size below 500 nm.

Based on the results and observations, it can be concluded that the bio-hybrid hydrogel matrices are stable materials and the presence of an additional component i.e. the thermosensitive carrier – the hydrocortisone system - does not reduce the degree of matrix cross-linking or its swelling ability. Moreover, the swelling tests results indicated that the systems containing the higher drug concentration had the slightly higher sorption capacity in both the tested immersion media. The FT-IR spectra of the bio-hybrid systems confirmed no changes in the structure associated with the presence of encapsulated polymeric carriers.

The conducted research is a good experimental basis for further investigations aimed at developing a novel third-generation bio-hybrid dressing system. The main goal of the project will be preparing the bio-hybrid hydrogel materials enhanced with the nanocarrier-drug system with the controlled drug release as an innovative way of treating *Psoriasis* - a serious skin disease with autoimmune background. The expected positive results, especially regarding non-toxicity, will enable the selection of a prototype and further work on the novel bio-hybrid hydrogel materials to improve wound healing.





References

- [1] Yucan W., Hui C., Xinying W.: Synthesis and characterization of an injectable ϵ -polylysine/carboxymethyl chitosan hydrogel used in medical application. *Materials Chemistry and Physics* 248 (2020) 122902.
- [2] Cheng J., Jia Z., Li Teng.: A constitutive model of microfiber reinforced anisotropic hydrogels: With applications to wood-based hydrogels. *Journal of the Mechanics and Physics of Solids* 138 (2020) 103893.
- [3] Kamoun E.A., Kenawy E.R.S., Chen X.: A review on polymeric hydrogel membranes for wound dressing applications: PVA-based hydrogel dressings. *Journal of Advanced Research* 8 (2017) 217-233.
- [4] Singh T.R.R., Laverty G., Donnelly R.: *Hydrogels. Design, Synthesis and Application in Drug Delivery and Regenerative Medicine*, 1 edition, CRC Press 2018.
- [5] Ver Halen J., Naylor T., Petersen D.K.: Current and future applications of nanotechnology in plastic and reconstructive surgery. *Plastic and Aesthetic Research* 1 (2014) 43-50.
- [6] Ding M., Jing L., Yang H., Mechanicki C.E., Fu X., Li K., Wong I.Y., Chen P.-Y.: Multifunctional soft machines based on stimuli-responsive hydrogels: from freestanding hydrogels to smart integrated systems. *Materials Today Advances* 8 (2020) 100088.
- [7] Bialik-Wąs K., Pluta K., Malina D., Majka T.M.: Alginate/PVA-based hydrogel matrices with *Echinacea purpurea* extract as a new approach to dermal wound healing. *International Journal of Polymeric Materials and Polymeric Biomaterials*, article in press, DOI: 10.1080/00914037.2019.1706510
- [8] Nlemirowicz K., Car H.: Nanocarriers as modern transporters in the controlled delivery of drugs. *CHEMIK* 66 (2012) 868-881.
- [9] Vauthier C., Bouchemal K.: Methods for the preparation and manufacture of polymeric nanoparticles. *Pharmaceutical Research* 26 (2009) 1025-1058.
- [10] Chaudhari A.A., Vig K., Baganizi D.R., Sahu R., Dixit S., Dennis V., Singh S.R., Pillai S.R.: Future Prospects for Scaffolding Methods and Biomaterials in Skin Tissue Engineering: A Review. *International Journal of Molecular Sciences* 17 (2016) 1974.
- [11] Utech S., Boccaccini, A.R.: A review of hydrogel-based composites for biomedical applications: enhancement of hydrogel properties by addition of rigid inorganic fillers. *Material Science* 51 (2016) 271-310.
- [12] Ma M., Zhong Y., Jiang X.: Thermosensitive and pH-responsive tannin-containing hydroxypropyl chitin hydrogel with long-lasting antibacterial activity for wound healing. *Carbohydrate Polymers* 236 (2020) 116096.
- [13] Fan H., Wang J., Zhang Q., Jin Z.: Tannic Acid-Based Multifunctional Hydrogels with Facile Adjustable Adhesion and Cohesion Contributed by Polyphenol Supramolecular Chemistry. *ACS omega* 2 (2017) 6668-6676.
- [14] Kang W., Bi B., Zhuo R., Jiang X.: Cytocompatible and non-fouling zwitterionic hyaluronic acid-based hydrogels using thiol-ene "click" chemistry for cell encapsulation. *Carbohydrate Polymers* 236 (2020) 18-25.
- [15] Nesović K., Janković A., Radetić T., Perić-Grujić A., Vukašinović-Sekulić M., Kojić V., Rhee K.Y., Mišković-Stanković V.: Poly(vinyl alcohol)/chitosan hydrogels with electrochemically synthesized silver nanoparticles for wound dressing applications. *European Polymer Journal* 121 (2019) 109257.
- [16] Zheng L.Y., Zhu J.F.: Study on Antimicrobial Activity of Chitosan with Different Molecular Weights. *Carbohydrate Polymers* 54 (2003) 527-530.
- [17] Durian N., Durian M., Bispo de Jesus M., Seabra A.B., Fávaro W.J., Nakazato G.: Silver nanoparticles: A new view on mechanistic aspects on antimicrobial activity. *Nanomedicine: Nanotechnology, Biology, and Medicine* 12 (2016) 789-799.
- [18] Simpson E.L.: Atopic dermatitis: a review of topical treatment options. *Current Medical Research and Opinion*, 26 (2010), 633-640.
- [19] Harrison I.P., Spada F.: Hydrogels for atopic dermatitis and wound management: a superior drug delivery vehicle. *Pharmaceuticals*, 10 (2018), 71.
- [20] Szcześniak M., Grimling B., Meler J., Karolewicz B.: Application of chitosan in the formulation of dermatological hydrogels prepared on the basis of macromolecular compounds, *Progress on Chemistry and Application of Chitin and its Derivatives*, Volume XXIII, 2018.
- [21] Shufan Chen, Xiaodong Jiang, Lianlai Sun: Reaction Mechanisms of N-isopropylacrylamide soap-free emulsion polymerization based on two different initiators. *Journal of Macromolecular Science, Part A*, 51:5 (2014) 447-455.
- [22] Patent application no. P.432720: Method of obtaining dressing material (2020)
- [23] Silverstein R.M., Webster F.X., Kiemle D.J.: *Spectrometric Identification of Organic Compounds*, John Wiley & Sons, Inc, New York 2005.
- [24] Pereira R., Tojeira A., Vaz D.C., Mendes A., Bártoło P.: Preparation and Characterization of Films Based on Alginate and Aloe Vera. *International Journal of Polymer Analysis and Characterization* 16 (2011) 449-464.
- [25] Koga A.Y., Pereira A.V., Lipinski L.C., Oliveira M.R.P.: Evaluation of wound healing effect of alginate films containing *Aloe vera* (*Aloe barbadensis Miller*) gel. *Journal of Biomaterials Applications*. 32(9) (2018) 1212-1221.
- [26] Kim M.H., Kim J.C., Lee H.Y., Kim J.D., Yang J.H.: Release property of temperature-sensitive alginate beads containing poly(N-isopropylacrylamide). *Journal of Colloids and Surface B* 46 (2005) 57-61.









Acknowledgments

This research was supported by The National Centre for Research and Development – project LIDER/41/0146/L-9/17/NCBR/2018.

ORCID iDs

- D. Malina:  <https://orcid.org/0000-0001-8539-4368>
 E. Królicka:  <https://orcid.org/0000-0001-7812-0887>
 K. Bialik-Wąs:  <https://orcid.org/0000-0002-1757-9499>
 K. Pluta:  <https://orcid.org/0000-0001-9366-2473>

ORGANIC BACTERIOSTATIC MATERIAL

TOMASZ FLAK^{1,2} , JAROSŁAW PALUCH³ ,
JADWIGA GABOR² , HUBERT OKŁA² ,
ARKADIUSZ STANULA⁴ , JAROSŁAW MARKOWSKI³ ,
JAN PILCH³ , ANDRZEJ SZYMON SWINAREW^{2,4*} 

¹ POLYMERTECH LTD.

75 PUŁKU PIECHOTY 1, 41-500 CHORZÓW, POLAND

² FACULTY OF SCIENCE AND TECHNOLOGY,

UNIVERSITY OF SILESIA IN KATOWICE,

75 PUŁKU PIECHOTY 1A, 41-500 CHORZÓW, POLAND

³ DEPARTMENT OF LARYNGOLOGY,

SCHOOL OF MEDICINE IN KATOWICE,

MEDICAL UNIVERSITY OF SILESIA IN KATOWICE, POLAND

UL. MEDYKÓW 18, 40-752 KATOWICE, POLAND

⁴ DEPARTMENT OF INDIVIDUAL SPORTS,

INSTITUTE OF SPORT SCIENCE,

THE JERZY KUKUCZKA ACADEMY OF PHYSICAL EDUCATION,

MIKOŁOWSKA 72A, 40-065 KATOWICE, POLAND

*E-MAIL: ANDRZEJ.SWINAREW@US.EDU.PL

Abstract

The use of antibiotics to treat bacterial infections is becoming less and less effective year by year due to the increasing resistance of bacteria. The microbial evolutionarily acquired resistance to antibiotics increases the threat to man's life due to difficulties regarding effective therapies to fight infections. Therefore, apart from treatment, it is necessary to introduce appropriate prophylaxis which limits the multiplication of bacterial colonies on everyday use objects. Due to the antibiotic resistance phenomenon, it is important to find a new material with antibacterial properties for FDM 3D printing in medical applications.

The work contains research on a new chemical compound used as an additive to thermoplastics. The rhodamine derivative was synthesized via the 4-diphenylaminobenzaldehyde reaction with 1.3-indendione in a boiling mixture of EtOH/H₂SO₄. The obtained chemical compound was used as a bacteriostatic modifier of the polycarbonate (PC) properties, as such a modification enables application e.g. for medical device housings or for surfaces frequently touched by people.

The modifier and the commercially available polymer were compounded with a high-temperature screw extruder and a filament for FDM 3D printer was created. The modified polymer revealed antibacterial properties relative to Escherichia coli and good thermal stability during the processing.

Keywords: bacteriostatic, rhodamine, polymer, Escherichia Coli

[Engineering of Biomaterials 155 (2020) 17-21]

doi:10.34821/eng.biomat.155.2020.17-21

Introduction

In this study, we present the method of obtaining a new bacteriostatic material and its practical applications. Commercially available polymers, in most cases, are not biodegradable. Some of those plastics can biodegrade over time but it is a phenomenon of the irrelevant scale. Low biodegradation potential is connected with low susceptibility to degradation by fungi, bacteria, or mites and high resistance to most of the solvents. The aforementioned properties should provide conditions inhibiting the development of microbial colonies due to low nourishment availability. However, in everyday situations, most materials are covered with contaminants, such as tallow, food debris, or dust, which create a friendly environment for bacteria. In most cases, this phenomenon does not have a major impact on the material applicability, but in medical and personal hygiene products (syringes, toothbrushes, shower cabins) as well as other personal items (headphones, mobile phone cases) bacteriostatic properties become a very desirable feature.

Due to the increasing resistance of bacteria, the use of antibiotics in the fight against microbial infections is becoming less and less effective year by year [1-3]. The evolutionarily acquired resistance to antibiotics increases the threat to man's life due to difficulties regarding effective infection treatment. Therefore, it is necessary to introduce appropriate prophylaxis which limits the multiplication of bacterial colonies on everyday use objects.

Currently, the most commonly used methods of limiting bacterial growth on the materials surface are sterilization and creating a protective surface that contains nano additives. As a result of sterilization, bacterial colonies are removed, but this effect usually does not last as there is no additional long-term antimicrobial protection. In case of contamination of a newly sterilized surface, it quickly becomes a potential friendly environment for the bacteria growth. A new way to decrease the bacteria population is protection based on nanoparticles. Nowadays, nanosilica and nanosilver are in the spotlight as potential antibacterial substances [4-5]. However, there are still some apprehensions concerning the safety of using nanomaterials [6] and this solution is far from perfect.

Unfortunately, microbes have an evolutionary ability to adapt to new disinfectants. Therefore, it is reasonable to continuously look for new methods to limit their proliferation. Rhodamine B and its derivatives can be a great alternative to nanomaterials as well as thermal or chemical sterilization [7]. Rhodamine B is a red-purple compound with the chemical formula C₂₈H₃₁ClN₂O₃ and one of the most important water-soluble organic dyes (FIG. 1).

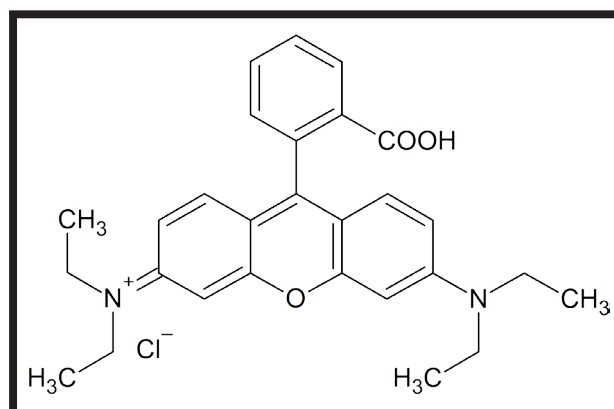


FIG. 1. Rhodamine B structure.

It is a very useful compound with properties supporting its application as a chromogenic reagent. Rhodamine B can also be used as a fluorescent sensor, e.g. it to detect glutathione [8], Cu^{2+} ions and 1-methionine. Rhodamine B and its derivatives have also found many applications in the chemical industry, for instance in the production of a polyvinyl chloride membrane that is able to detect mercury ions [9]. In this research, we synthesized a new derivative of rhodamine B endowed with bacteriostatic properties. However, unlike rhodamine B, the obtained compound is insoluble in water. Due to this advantageous property, a plastic additive is not susceptible to the compound washout. What is more, there is no increase in the hydrophilic properties of plastic, which is likely to occur while using water-soluble compounds as additives.

Materials and Methods

Pure ethanol (CAS number 64-17-5), 4-(diphenylamino)benzaldehyde 97% (CAS number 4181-05-9) and 1,3-indandione 97% (CAS number 606-23-5) was purchased at Sigma Aldrich. Sulphuric acid solution 95% a.a. (CAS number 7664-93-9) was purchased from Linegal Chemicals. Makrolon® 2407 polycarbonate was purchased from Covestro.

The synthesis scheme of the rhodamine derivative is shown in FIG. 2. In a 250 mL three-necked flask, under an inert atmosphere, 20 mL of anhydrous ethanol was mixed with a droplet of sulphuric acid to obtain an acidic ionic reaction medium. Then 2.00 g (7.33 mM) of 4-(diphenylamino)benzaldehyde and 0.52 g (3.5 mM) of 1,3-indandione were added to the mixture.

The resulting suspension was purged with argon 5.0 for 15 min. After that the reaction system was equipped with a magnetic dipole and brought to reflux under an inert gas atmosphere, being stirred vigorously for 24 h. The mixture turned brightly red. Then it was cooled to room temperature and the desired product was isolated using the SiO_2 column chromatography. A mixture of hexane and methylene chloride in gradient concentration was used as a mobile phase. The product was vacuum dried to solid weight and recrystallized from chloroform.

The filament for the 3D FDM printing was obtained in a homogenizer equipped with a Teflon mechanical stirrer. There the previously obtained 700 g of Makrolon® 2407 polycarbonate in the form of granules and 0.2 g of the dried bacteriostatic rhodamine modifier were mixed until the homogeneous polymers surface was covered by the rhodamine derivative. The surface-modified granulate was dried for 24 h at 100°C . In the next step, a 2.7 mm diameter string was made at temperatures: 180, 200, 210 and 225°C in subsequent heating zones within a four-zone single-screw extruder. Plates for analysis of microbiological interactions were made of the obtained material with the 3D FDM technology, using the proprietary FDM system with a heated 600 W table. During the process, the temperature of 285°C was maintained on the print-head and 165°C - on the table.

The evaluation of the antibacterial activity of the modified polycarbonate surface was carried out in accordance with the standard method [10]. The bacterial strain: *Escherichia coli* (ATCC® 25922) was used as the reference material. The inoculum volume at $6 \cdot 10^5$ cells/mL was 0.4 mL.

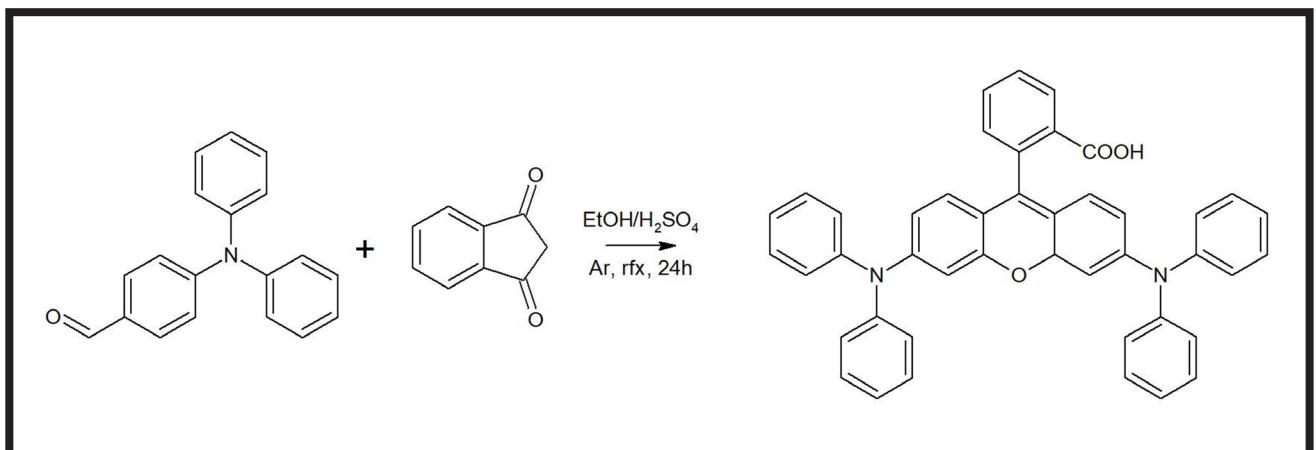


FIG. 2. Synthesis of rhodamine derivative - [9-(2-carboxyphenyl)-6-diphenylamino-3-xanthenylidene]-diphenylammonium.

TABLE 1. The antibacterial activity test parameters.

Parameter	Value
Control sample length x width x thickness	50x50x2.4 mm
Test sample length x width x thickness	50x50x2.4 mm
Cover film	Polypropylene foil 40x40x0.05 mm
Bacterial species and strain	<i>Escherichia Coli</i> , ATCC 25922
Inkulum volume	0.4 mL
Bacterial cell concentration	$6 \cdot 10^5$ cells/mL
Volume and type of neutralizer	10 mL, SCDLP broth
Study time	72 h

All the culture media and solutions were prepared according to the standard method [10]. The parameters of the antibacterial activity are given in TABLE 1. The coefficient of antibacterial activity (R) of the tested material was determined according to the formula (1):

$$R = (U_t - U_0) - (A_t - U_0) = U_t - A_t$$

where: U_0 is the average logarithm of the number of live bacteria recovered from the untreated samples after plating, number of cells/cm²; U_t means the decimal logarithm of the number of live bacteria recovered from untreated samples after 24 h, number of cells/cm²; and A_t is the average logarithm of the live bacteria number recovered from the samples treated after 24 h, the number of cells/cm².

The MALDI –ToF analysis was carried out to determine the structure of the obtained rhodamine derivative. The spectra were obtained on AXIMA Performance instrument using graphite as a matrix material for those analyses.

The FTIR tests were carried out using the Shimadzu IR Tracer spectrophotometer equipped with the ATR multi-reflection device. The sample was applied directly to the ATR. The measurement parameters were 100 scans for each sample.

Results and Discussions

The new compound was synthesized through the reaction mechanism shown in FIG. 3.

The structure of the obtained additive was confirmed with the MALDI – ToF analysis (FIG. 4). On the mass spectra, the rhodamine derivative was recorded as an adduct with the potassium ion. In this case, the intensity did not determine the compound amount, but only the ionization method did.

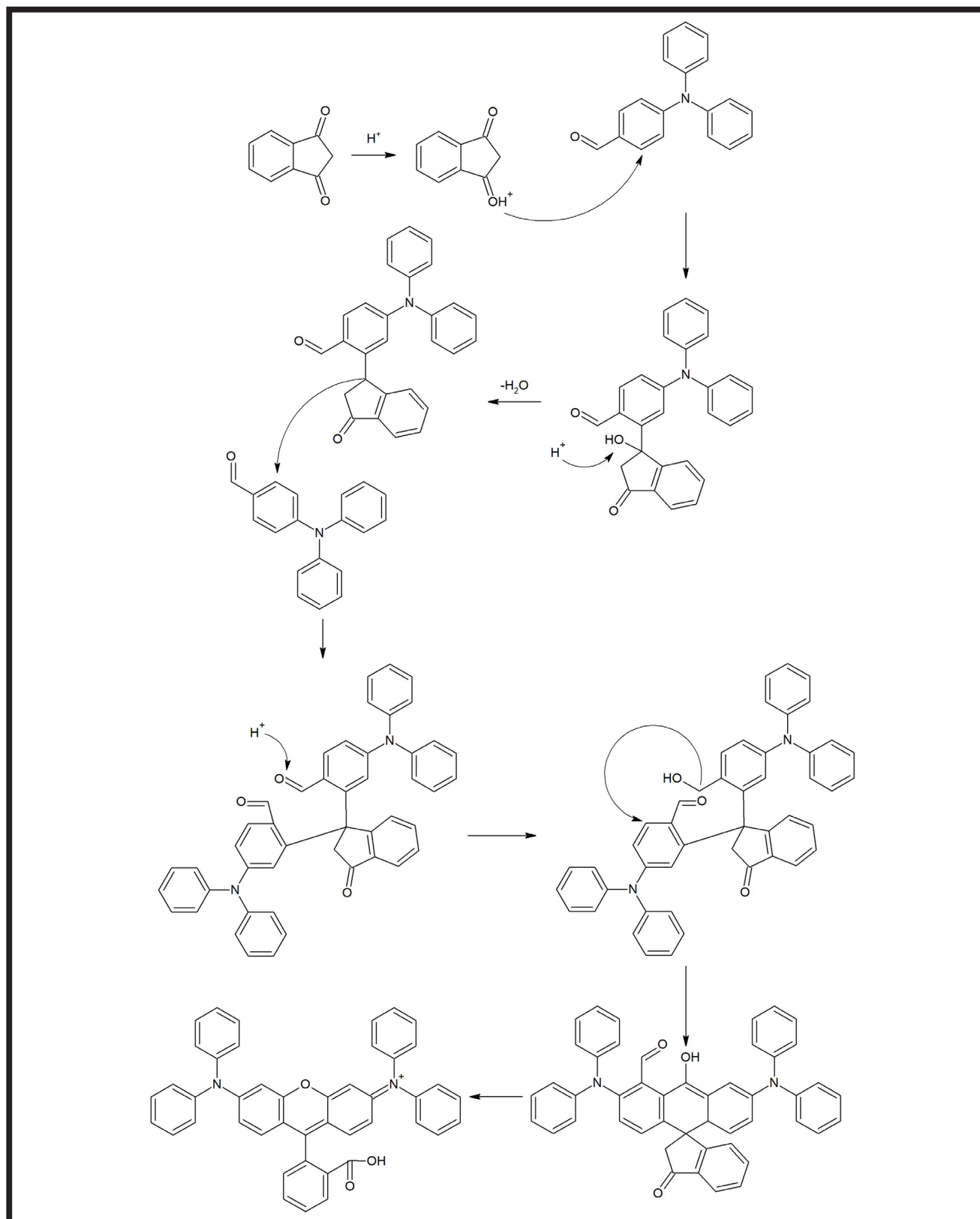


FIG. 3. The proposed reaction mechanism.

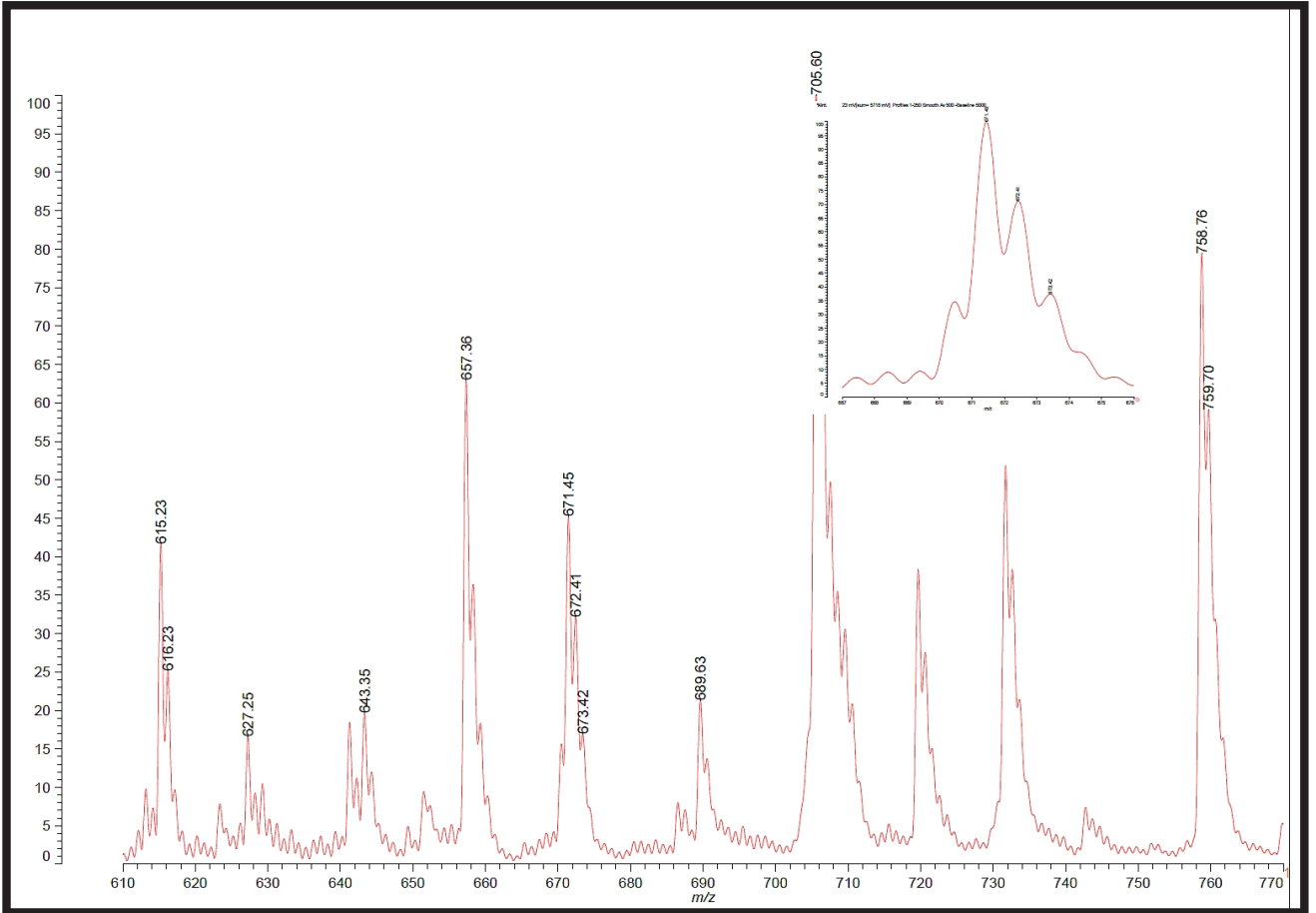


FIG. 4. The MALDI -ToF spectra of rhodamine derivative - additive.



FIG. 5. Evolution of the IR spectra during thermal processing of the composite compared with pure polycarbonate. PC – black (1), modified granules – red (3), modified material printout from 3D printer – green (2).

Therefore, some impurities and residues of the reaction mixture had a higher intensity than the registered adduct of the rhodamine B derivative with potassium ion.

The obtained additive was used as a polycarbonate modifier and for 3D printing.

Comparing the obtained IR spectra for the pure material (PC), the modified granules and the sample after the thermal treatment – the 3D printing (FIG. 5.), the appearance of new bands was not noticed. Therefore, it may be concluded that the thermal treatment did not adversely affect the material.

It was observed that the polymers potential to form the biofilm on the product's surface decreased. The test results are presented in TABLE 2. The determined coefficient of antibacterial activity R indicated the bacteriostatic properties of the material in relation to the reference strain *E. coli* specified in the standard.

Conclusions

The novel potentially bacteriostatic plastic modifier was synthesized. The obtained chemical compound proved that the rhodamine derivative may be used as an additive in plastics in the processing of high-temperature polycarbonate. Based on the applied low concentration and the high temperatures required for polycarbonate processing, it is assumed that this additive is also applicable for modifications of other thermoplastics. Moreover, the insolubility in water increases its potential as an addition to plastics. The authors are planning to perform a series of tests on the developed prototype material using 3D printing. Further work is also recommended to determine the mechanism of antibacterial activity of the obtained rhodamine derivative. The structure of the rhodamine B derivative was confirmed spectroscopically (FIG. 3). Even if further analysis should be carried out, it was already revealed that the examined material can be used to create surfaces limiting the bacterial biofilm formation.

TABLE 2. The antibacterial activity test results.

Parameter	Value
U_0	4.21
U_t	4.91
A_t	3.46
R	1.45









The comparative analysis results proved all the tested materials to be suitable for filaments in the FDM 3D printing. The compatibility between polycarbonate and its additive was also demonstrated. No surface changes, inclusions or agglomeration of the additive were observed during the material preparation and processing.

Future studies of this material are planned in order to define the mechanism of antibacterial activity more accurately.

Acknowledgments

Work co-funded from statutory research KNW-1-142/N/9/0 and KNW-1-133/N/8/0.

ORCID iDs

T. Flak:	 https://orcid.org/0000-0003-1300-6981
J. Paluch:	 https://orcid.org/0000-0001-7675-0623
J. Gabor:	 https://orcid.org/0000-0003-4850-1608
H Okla:	 https://orcid.org/0000-0001-7210-2995
A. Stanula:	 https://orcid.org/0000-0003-1759-6456
J. Markowski:	 https://orcid.org/0000-0003-3416-7354
J. Pilch:	 https://orcid.org/0000-0002-2682-4708
A. Swinarew:	 https://orcid.org/0000-0001-6116-9510

References

- [1] Høiby N., Bjarnsholt T., Givskov M., Molin S., Ciofu O.: Antibiotic resistance of bacterial biofilms. *Int J Antimicrob Agents* 35(4) (2010) 322-332. doi:10.1016/j.ijantimicag.2009.12.011
- [2] Novo A., André S., Viana P., Nunes O.C., Manaia C.M.: Antibiotic resistance, antimicrobial residues and bacterial community composition in urban wastewater. *Water Res.* 47(5) (2013) 1875-1887. doi:10.1016/j.watres.2013.01.010
- [3] Dafale N.A., Semwal U.P., Rajput R.K., Singh G.N.: Selection of appropriate analytical tools to determine the potency and bioactivity of antibiotics and antibiotic resistance. *J Pharm Anal.* 6(4) (2016) 207-213. doi:10.1016/j.jpha.2016.05.006
- [4] Bakhsheshi-Rad H.R., Hamzah E., Kasiri-Asgarani M., Saud S.N., Yaghoobidoust F., Akbari E.: Structure, corrosion behavior, and antibacterial properties of nano-silica/graphene oxide coating on biodegradable magnesium alloy for biomedical applications. *Vacuum* 131 (2016) 106-110.
- [5] Li L., Zhao C., Zhang Y., et al. Effect of stable antimicrobial nano-silver packaging on inhibiting mildew and in storage of rice. *Food Chem.* 215 (2017) 477-482. doi:10.1016/j.foodchem.2016.08.013
- [6] Scientific Committee on Emerging and Newly Identified Health Risks SCENIHR, Opinion on nanosilver. Safety, health and environmental effects and role in antimicrobial resistance, 10-11 June 2014 r., European Union, 2013 ISSN 1831-4783, ISBN 978-92-79-30132-2, doi:10.2772/76851 ND-AS-13-002-EN-N.
- [7] Bucki R., Pastore J.J., Randhawa P., Vegners R., Weiner D.J., Janmey P.A.: Antibacterial activities of rhodamine B-conjugated gelsolin-derived peptides compared to those of the antimicrobial peptides cathelicidin LL37, magainin II, and melittin. *Antimicrob Agents Chemother.* 48(5) (2004) 1526-1533. doi:10.1128/aac.48.5.1526-1533.2004
- [8] Xiaolei Wu, Hai Shu, Baojing Zhou, Yougliang Geng, Xiaofeng Bao, Jing Zhu: Design and synthesis of a new rhodamine B-based fluorescent probe for selective detection of glutathione and its application for live cell imaging, *Sensors and Actuators B: Chemical* 237 (2016) 431-442. doi:10.1016/j.snb.2016.06.161.
- [9] Li Yi, Zhang Zhou-Na, Ca Wei, Gao Xiao-Meng, Wang Beng: Mercury ion selective light addressable potentiometric sensor based on PVC membrane. *Zhejiang DaxueXuebao (Gongxue Ban)/Journal of Zhejiang University (Engineering Science)* 44 (2010) 1231-1236. doi:10.3785/j.issn.1008-973X.2010.06.033.
- [10] ISO 22196:2007(E), Plastics. Measurement of antibacterial activity on plastics surfaces.

LASER MODIFIED FUNCTIONAL CARBON-BASED COATINGS ON TITANIUM SUBSTRATE FOR CARDIAC TISSUE INTEGRATION AND BLOOD CLOTTING INHIBITION

ROMAN MAJOR^{1*} , ROMAN OSTROWSKI² , MARCIN SURMIAK³ , KLAUDIA TREMBECKA-WÓJCIGA¹ , JUERGEN LACKNER⁴ 

¹ INSTITUTE OF METALLURGY AND MATERIALS SCIENCE, POLISH ACADEMY OF SCIENCES, REYMONTA STR. 25, 30-059 KRAKOW, POLAND

² MILITARY UNIVERSITY OF TECHNOLOGY, INSTITUTE OF OPTOELECTRONICS, GEN. S. KALISKIEGO STR. 2, 00-908 WARSAW, POLAND

³ DEPARTMENT OF INTERNAL MEDICINE, JAGIELLONIAN UNIVERSITY MEDICAL COLLEGE, SKAWINSKA STR. 8, 31-066 KRAKOW, POLAND

⁴ JOANNEUM RESEARCH FORSCHUNGSGES MBH, INSTITUTE OF SURFACE TECHNOLOGIES AND PHOTONICS, FUNCTIONAL SURFACES, LEOBNER STRASSE 94, A-8712 NIKLASDORF, AUSTRIA

*E-MAIL: R.MAJOR@IMIM.PL

Abstract

The work focused on developing functional coatings on titanium substrates that would facilitate the integration with the cardiac tissue and with a specific form of connective tissue like blood. Surface modifications consisted in the laser evaporation of part of the biocompatible layer, thus creating a suitable environment for a particular tissue. For the myocardium integration, the metal surface was refined by biohemocompatible coatings. Such surfaces were the starting point for further modifications in the form of channels. The channeled surfaces enabled a controlled cell migration and proliferation. The interaction of endothelial cells with the material was highly dependent on the surface characteristics such as: topography, microstructure or mechanical properties. The controlled cellular response was achieved by modifying the surface to obtain a network of wells or channels of different dimensions via the laser interference lithography. This technique determined a high resolution shape, size and distribution patterns. As a result, it was possible to control cells in the scale corresponding to biological processes. The surface periodization ensured the optimal flow of oxygen and nutrients within the biomaterial, which was of a key importance for the cell adhesion and proliferation. The work attempted at producing the surface networks mimicking natural blood vessels. To stimulate the formation of new blood vessel the finishing resorbable synthetic coatings were applied on the surface to act as a drug carrier. Therefore, the initial trial to introduce factors stimulating the blood vessels growth was performed.

Keywords: thin layers, migration channels, laser ablation, microstructure

[*Engineering of Biomaterials* 155 (2020) 22-31]

doi:10.34821/eng.biomat.155.2020.22-31

Introduction

Engineering of biomaterials requires a thorough understanding of the cell-material interaction. The aim of our project was to modify the material surface for application in the cardiovascular system regeneration, namely to solve a problem of the cardiac tissue integration with a metallic element. The main limitation in the *in vitro* tissue engineering is the lack of a sufficient blood vessel system — the vascularization [1]. *In vivo* a highly developed system of larger blood vessels which are subdivided into small capillaries supplies nearly all tissues with nutrients and oxygen. In the case of artificial materials, the spontaneous vascular ingrowth occurs after implantation, yet it is often limited to several tenths of micrometers per day. It means that the time necessary to complete the implant vascularization is measured in weeks. During this time, insufficient vascularization may lead to nutrient deficiencies or hypoxia deeper in the tissue. Moreover, nutrient and oxygen gradients are present in the outer tissue regions only, resulting in the non-uniform cell differentiation and integration. In consequence of all these phenomena the tissue functionality decreases. Therefore, additional strategies enhancing the proper vascularization are essential. Current strategies to create vascularized tissues are discussed in this review [1]. The paper describes the endothelial cells and their neoangiogenesis, i.e. the ability to form new vessels. The pre-vascularization techniques are compared to the biomolecules approach where growth factors, cytokines, peptides and proteins and cells, are applied to generate new vessels. Biomaterials are engineered to promote endothelial cell adhesion and proliferation. There are several explanations of the cellular response to the applied carrier based on the synergistic effect of the material mechanical properties and the presence of bioactive molecules. Metallic biomaterials are popular for cardiac usage due to their inertness and structural functions. The high strength and resistance to fracture promote their use for cardiovascular regeneration e.g., artificial heart valves, components of heart assist devices, vascular stents [2]. Commonly used biocompatible metals include titanium, stainless steel, gold and silver. The increased interest in titanium and its alloys as biomaterials comes from their high corrosion resistance and good mechanical properties. However, their main drawback is low potential to cellularization and low hemocompatibility. To solve this problem the surface modification of titanium scaffolds is required. According to the literature, modulation of surface parameters like topography, chemistry or microstructure have a direct influence onto the cellular response [1-4]. The architecture and design of a scaffold have a profound effect on the endothelial cell adhesion and the vascularization rate. Moreover, the topography of the scaffold is a critical determinant of the blood-vessel ingrowth. Druecke et al. showed that the vessel ingrowth was significantly faster in periodical structured scaffolds [3]. The latest reports have shown that effective vascularization in tissue engineering is inherently linked to the intelligent scaffold design [3]. For this purpose, the ability to maintain suitable oxygen tensions and nutrient diffusion throughout the scaffold is critical. One of the ways that has been addressed is the use of channeled scaffolds. Alison P. McGuigan and Michael V. Sefton et al. [4] pointed out that endothelial cells are used in combination with biomaterials in a number of applications for the purpose of improving blood compatibility and host integration. Endothelialized vascular grafts are already used clinically with some success, while the endothelial seeding is being explored as a mean of creating the vasculature within engineered tissues. That's why surface engineering plays a significant role in the cell-material interaction. The details are presented elsewhere [5].

The interaction of cells and tissues with artificial materials designed for applications in medical biotechnology is governed by the physical and chemical properties of the material surface. Nanostructured substrates (i.e. substrates with irregularities smaller than 100 nm) are generally considered to be beneficial for the cell adhesion and growth, while microstructured substrates behave more controversially. According to the literature [6-15], micropatterned surfaces enable the regionally selective cell adhesion and directed growth, which can be utilized in tissue engineering, in constructing microarrays and in biosensors. Nanopatterned surfaces are an effective tool for manipulating the type, number, spacing and distribution of ligands for the cell adhesion receptors on the material surface. As a consequence, these surfaces are able to control the size, shape, distribution and maturity of focal adhesion plaques on cells, and thus the cell adhesion, proliferation, differentiation and other cell functions. Control of cell phenotype involves a variety of signalling pathways and transcriptional regulators. This multifunctional signalling molecule is part of adhesion contacts in the endothelium and is able to translocate into the nucleus to activate genetic programs and control proliferation and the fate of the cells. Micropatterning can precisely reconstruct the spatial and temporal features of the cellular microenvironment. This technique represents one of the most effective, high-precision method to modify two main surface properties (topography and micro-structure) [16-18]. Laser interference lithography, consisting in the creation of organized periodical surfaces based on selective material ablation, offers the possibility to create 2D and 3D patterns on surfaces. This technique enabled the precise control of the pattern shape, size and distribution. Materials structuration has found application in the cardiovascular materials engineering field. The surface lithography permitting control of cellular behaviors at scales matching those of biological processes. Using this method Marczak et al [19] were able to control the cell behaviour on the DLC layer deposited onto the silicon substrate. Biomaterials dedicated for direct blood contacting purpose require the design of fully atombogenic surface which do not adverse interact with any blood components [20]. This represents a really complex task due to a variety of processes occurring within this interface, including plasma protein adsorption, cell adhesion, and activation followed by thrombus formation [21]. Proteins mediate between the surface cell adhesion (e.g. fibrinogen) or can form a non-adhesive layer (e.g., albumin). Thus, controlling their selective adsorption to the surface is a key issue in hemocompatible materials design. A complete, tenaciously-adherent protein layer is formed within 5 seconds after the biomaterial exposure to blood flow [22]. Such a layer formation represents a dynamic and competitive process directly affecting the hemocompatible material properties because of different characteristics of specific proteins [22]. In literature, plasma proteins are divided into two main types: adhesive and non-adhesive ones [23-26]. The adhesive proteins (e.g., fibrinogen, fibronectin and von Willebrand Factor) tend to increase thrombosis by mediating platelet adhesion, while the non-adhesive ones (e.g., albumin, transferrin like proteins) can decrease subsequent thromboembolic events [24-26]. As the protein adsorption is the first step in a blood-solid state interaction, controlling the composition helps to improve hemocompatible properties of biomaterials. Over the past two decades, many studies have shown that the plasma protein adsorption followed by the platelet adhesion and activation is reduced on the albumin-coated biomaterial surfaces [25-26]. What is more, the adsorbed layer may minimize the adhesion of bacteria to biomaterials due to the lack of albumin/bacteria interaction [26]. This inspired researchers to develop new methods to obtain albumin-coated

passive materials by selective albumin adsorption to the surface in a blood environment. However, it has not been described yet how the surface features affect the albumin adsorption from blood in dynamic conditions. The hemodynamic conditions cause superficial stresses near the vessel wall (shear stresses) caused by blood flow inside vessels. Shear stresses may lead to the blood components conformational changes and the cells aggregation and thrombus. This carries serious consequences including blood clotting followed by the unhindered flows and resulting in the implant failure [27]. For this reason, it is important to fabricate the self-assembling material surfaces which enable the spontaneous formation of an albumin layer from the blood.

Materials and Methods

As part of the task, titanium alloy substrates were modified with thin amorphous carbon coatings (a-C:H) and subsidized with nanoparticles of various elements to improve the hemophilic properties. All surface modifications were made in cooperation with MATERIALS - Institute for Surface Technologies and Photonics. The first stage consisted in optimizing the surface modifications in terms of interactions with blood. Coatings were deposited using the Physical Vapour Deposition (PVD) technique. Prior to deposition, the substrates were ultrasound cleaned with ethanol and then dried under vacuum. After the substrates were installed in parallel to the target surface at a distance of ~120 mm, a vacuum chamber was used to achieve at least 4×10^{-3} Pa. Before the coating was deposited, an anode layer ion source was used. It is a method enabling etching and used to clean the surface from oxide layers. Next, a Direct Current (80 kHz pulsed 80 kHz, 2000 W, pyrolytic carbon with 99.95% C as a shield from Schunk, Bad Goisern, Austria) was used to deposit the a-C:H and a-C:N coatings in Ar and Ar+N₂ at 3×10^{-1} Pa, respectively. The application of hemophilic thin film materials was carried out in several stages, successively improving their properties. The deposition parameters of the first group of materials are shown in TABLE 1.

Carbon-based coatings were deposited on silicon wafers by means of physical steam deposition. Silicon substrates were selected deliberately because of their smooth surface which allows for a thorough analysis of the surface effect of a thin layer on the cell-material interaction, with particular emphasis on red blood cells. The substrate dimensions for all the tests were 1.5 cm x 1.5 cm. For hydrodynamic tests, the substrates had 14.4 mm in diameter of and no more than 0.5 mm in thickness. The size of the tested hydrodynamic sample was matched with the geometry of the tester vessels. The deposition process was performed at room temperature using an industrially scaled vacuum coating (manufacturer: Pfeiffer Vacuum, Asstar, Germany). The deposition parameters of the second group of materials are shown in TABLE 2.

Endothelial cells play a major role in the complex mechanism that has evolved to ensure balance in the circulatory system. The endothelial layer acts as a dynamic interface that actively regulates inflammation, thrombosis and fibrinolysis. A number of undesirable reactions may occur in the case of the blood contacting the surface. The endothelium is commonly known as the most biocompatible in contact with streaming blood. Its combination with biomaterials can be used to prevent thrombotic and inflammatory reactions and improve the integration with artificial materials. One of the milestones in the task was to achieve the full endothelial cells confluence by controlling the surface structuring. The local environment is of key importance for the cells behaviour, shape, alignment and orientation.

The substrate chemical composition and topography influence such cell functions as: adhesion, growth, motility, gene expression and apoptosis. Controlling the biological environment through the appropriate substrate properties is crucial tissue engineering. Biocompatibility and mechanical strength support the growth and contraction of tissues. Appropriate physical and chemical properties promote the cell adhesion and growth. Channels and ridges in the surface structure lead to the proper migration and orientation of cells, ensuring the healthy tissue organization and its mechanical strength. Currently, the most popular techniques for preparing 3D scaffolding are photolithography, soft lithography,

direct recording and laser ablation. Material and distribution constraints and high costs are disadvantages of photolithography, therefore the laser ablation method was used in the task to create migration channels. The advantages of this approach are: high resolution (up to 25 nm), non-contact interaction and applicability on any substrate. Thermal and mechanical propagation occurs during irradiation with nanosecond and longer laser pulses, causing melting and evaporation away from the absorption point and re-curing of the melting zone. The aim of the study was to structure the biomaterials surface with a laser beam to ensure the controlled migration of HUVEC (Human Umbilical Vein Endothelial Cells) cells. The presented results are of a cognitive nature in terms of the cell behavior depending on the substrate modification. This strategy has led to the generation of macroscopic pathways.

Migration channels were obtained via the laser ablation performed by the Optoelectronics Department of the Military University of Technology. Thin nanometric fragments of the 50 nm-long coating were removed to retain the half of the coating thickness. The process of ablation results from the interaction of the laser radiation (absorption and scattering) with the liquid ejected material. During the material surface treatment performed with the pulsed laser radiation of the proper power density (density of energy appropriate in time) the following phenomena occur: the radiation absorption and thermal or photochemical effects. The desired reflection requires a low level of radiation. Therefore, the excitation requires a large surface area of the laser beams intensity and low laser radiation absorption. The thickness of the evaporated layer depends on the material properties such as: optical, thermal and laser beam parameters, wavelength, power density, laser pulse duration.

Migration channels were formed as intersecting lines according to the scheme presented in FIG. 1. The task was performed in the Department of Optoelectronics of the Military University of Technology. The channels were designed especially to indicate the optimal pathways distance to the most effective overgrowth by endothelial cells. A diagram presenting the laser system used to make the channels is shown in FIG. 2.

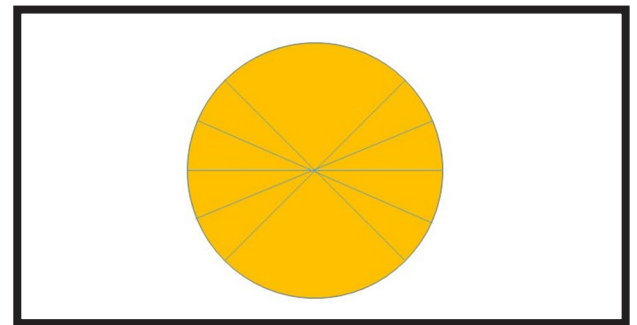


FIG. 1. Scheme of migration channels.

TABLE 1. Deposition parameters of the first series of materials.

C225_2: 125 nm Si – a-C:H	
Deposition	
Target material	Si
Power [kW]	2.5
Voltage [V]	Start: 623; End: 624
Current [A]	Start: 4.00; End: 3.99
Gas flow [sccm]	45 Ar + 5 C ₂ H ₂
Pressure [mbar]	2.3*10 ⁻³
Duration of the process [min]	7
Voltage Bias [V]	50 (DC)
Current Bias [mA]	180 – 350
Resolution [nm/min]	18.1 nm/min
C225_2: 15 nm Si – a-C:H	
Deposition	
Target material	Si
Power [kW]	2.5
Voltage [V]	Start: 629; End: 627
Current [A]	Start: 3.96; End: 3.97
Gas flow [sccm]	45 Ar + 5 C ₂ H ₂
Pressure [mbar]	2.4*10 ⁻³
Duration of the process [min]	1
Voltage Bias [V]	50 (DC)
Current Bias [mA]	180 – 270
Resolution [nm/min]	18.1 nm/min
C225_6: 100 nm a-C:H	
Deposition	
Target material	C
Power [kW]	3.0
Voltage [V]	Start: 580; End: 573
Current [A]	Start: 5.16; End: 5.22
Gas flow [sccm]	40 Ar + 10 C ₂ H ₂
Pressure [mbar]	2.2*10 ⁻³
Duration of the process [min]	19
Voltage Bias [V]	off
Current Bias [mA]	-
Resolution [nm/min]	5.48 nm/min

TABLE 2. Deposition parameters of the second series of materials.

Protokoll No. According to Table 1	Type of the coating			Thickness [nm]	Deposition process	Gas flow [sccm]
	a-C:H	a-C:H:N	a-C:H:Si			
Ti				0.0	sputter	-
C316_1	x			30	sputter	40.0 Ar + 10.0 C ₂ H ₂
C316_2		x		15	sputter	40.0 Ar + 2.5 C ₂ H ₂ + 7.5 N ₂
C316_3	x			100	sputter	40.0 Ar + 10.0 C ₂ H ₂
C316_4			x	125	sputter	24.0 Ar + 6.0 N ₂

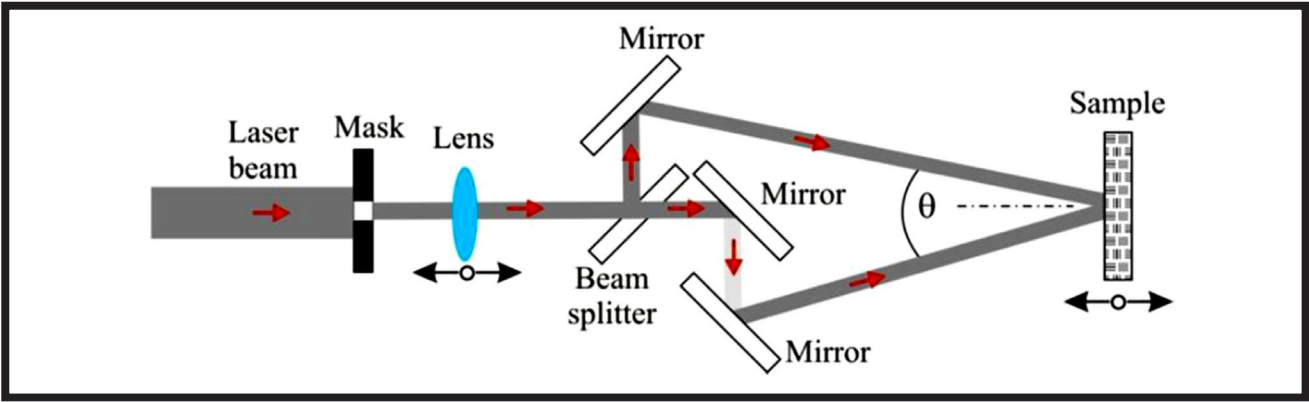


FIG. 2. Topography of migration channels at the lines intersection in the middle of the sample.

Results and Discussion

Characteristics of microstructure, chemical composition and mechanical properties. Studies on topography of migration channels are presented in FIGs. 3 i 4.

Microstructure

The self-inflicted stress distribution in the migration channels was performed using the X-ray diffraction method to measure the change of interplanar distance. The results of the stress distribution evaluation and the size of crystallites are presented in TABLES 3 and 4.

TABLE 3. The residual stress values in the designated places of the tested sample.

Area	Stress [MPa]	Standard deviation
Not modified	-6100.6	+/-300
Channel	-	-
Heat effective zone	-3500.5	+/-200
Area between the channels	-4600.2	+/-100

TABLE 4. The crystalline size values in the designated places of the tested sample.

Area	Size of crystallites Å
Not modified	96.4
Channel	116.3
Heat effective zone	96.0
Area between the channels	98.8

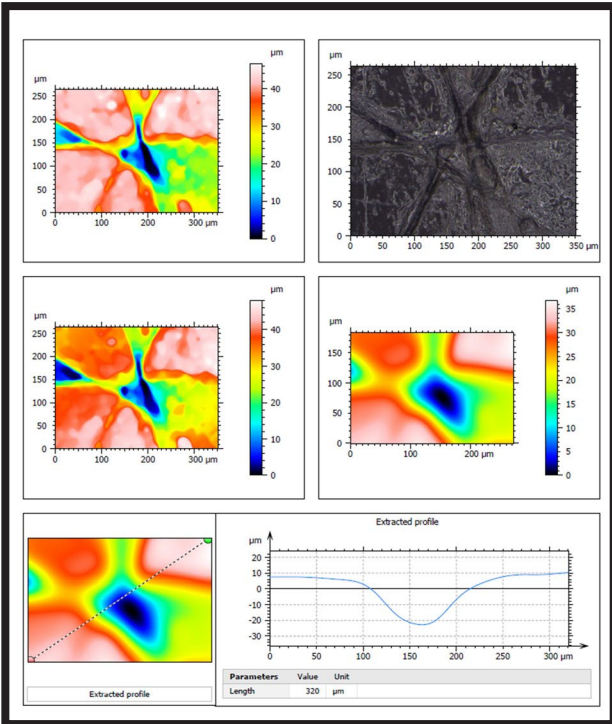


FIG. 3. Topography of migration channels at the lines intersection in the middle of the sample.

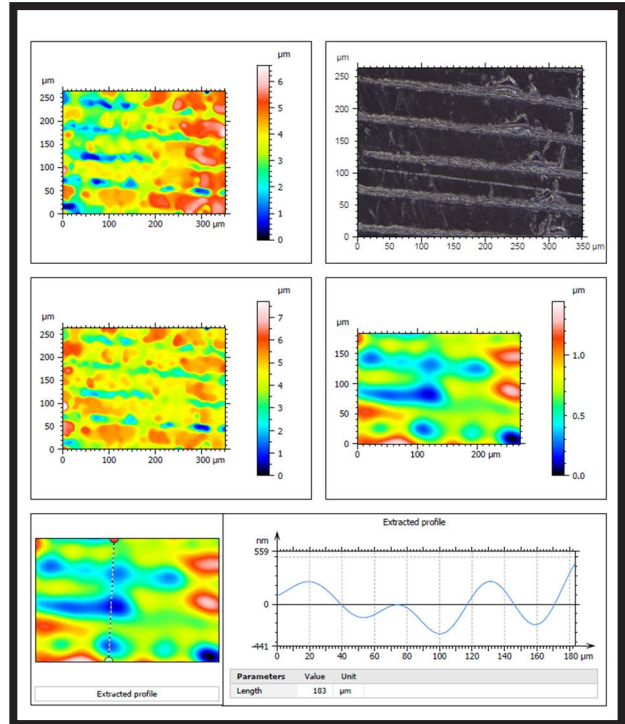


FIG. 4. Topography of migration channels at the edge of the sample.

The analysis of the migration channels structure was carried out using Transmission Electron Microscopy (TEM). For the TEM analysis thin films were prepared on the cross-section from the migration channel border to the unmodified surface. The platinum mask was used to differentiate the surface to be tested. The samples were made using the FIB (Focused Ion Beam Method) and the surface to be tested was marked on the SEM image. TEM was performed from the area at the tubule (FIG. 5) and in the tubule area (FIG. 6).

In vitro analysis

The influence of nano- and micro patterns on the adhesion, targeted growth and proliferation of endothelial cells was evaluated. The surface parameters were characterized to determine the proper formation of endothelial monolayer and blood vessel formation. The cell shape, contact surface, cell nucleus location, distribution of cytoskeleton elements (nucleus) and the number of adhesion molecules were compared. The expression of adhesion molecules, such as integrins, was transferred on the different stiffness and architecture materials. The cell migration process was observed on the structured surfaces. The hemophilic properties of surfaces and the protein adsorption to the substrates were analyzed using human blood. The analyses were carried out under conditions of high shear forces, simulating natural conditions in blood vessels. As a result of contact with the material, the degree of platelet and leukocyte activation in blood and the platelet aggregation were assessed.

Hemocompatibility test of a-C:H coatings

Hemocompatibility tests were carried out for the materials produced in the first phase of the project (TABLE 1). The aim of the experiment was to determine the biocompatibility in contact with blood and to select the materials for the final phase where the migration channels were made.

Two sets of tubes were prepared for each plate tested and for static control. Expression of platelet activation markers was determined by staining whole blood. In short, 5 μ L of blood was gently mixed with monoclonal antibodies conjugated with fluorochrome: 5 μ L FITC-PAC-1, 5 μ L PE-CD62P and 4 μ L PerCP-CD61 (all from Becton Dickinson, USA) in saline phosphate buffered (PBS) containing 0.2% bovine serum albumin and 2 mM calcium chloride (fi l. 35 μ L). After 10 minutes of staining at room temperature, erythrocytes were lysed by adding 0.5 mL of lysing solution (FLS, Becton Dickinson, USA) and the plates were centrifuged (1,000 g, 6 min) and resuspended in the PBS buffer for further analysis with the cytometry flow. The samples were analyzed with the EPICS XL flow cytometer (Beckman Coulter Inc., Brea, CA, USA). The expression of platelet activation markers was measured on CD61 gated objects using PAC-1 antibody to change the conformational glycoprotein IIb/IIIa and CD62P for P. The activation marker was calculated as the product of the sum of geometric fluorescence averages and the percentage of marker-positive objects. The platelet aggregates were analyzed after the erythrocytes analysis by mixing 25 μ L of blood with 0.4 mL FLS and then fixing them by adding 3.5 mL 1% paraformaldehyde in PBS. Cellular material was recovered by centrifugation (1,000 g, 7 minutes) and staining of active leukocytes (25 μ L portions) with 4 μ L PerCP-CD14 and 5 μ L FITC-CD61 or 5 μ L FITC-CD61 for 30 min at room temperature. The samples were then rinsed in PBS and subjected to the cytometric analysis. The percentage share of granulocyte platelet aggregates (leukocytes stained with CD61 platelet marker) was calculated using the forward/backward dispersion granulocyte gate and an additional CD14+ monocyte gate. The absolute number of platelets was calculated as the number of CD61 positive objects in relation to the total number of granulocytes.

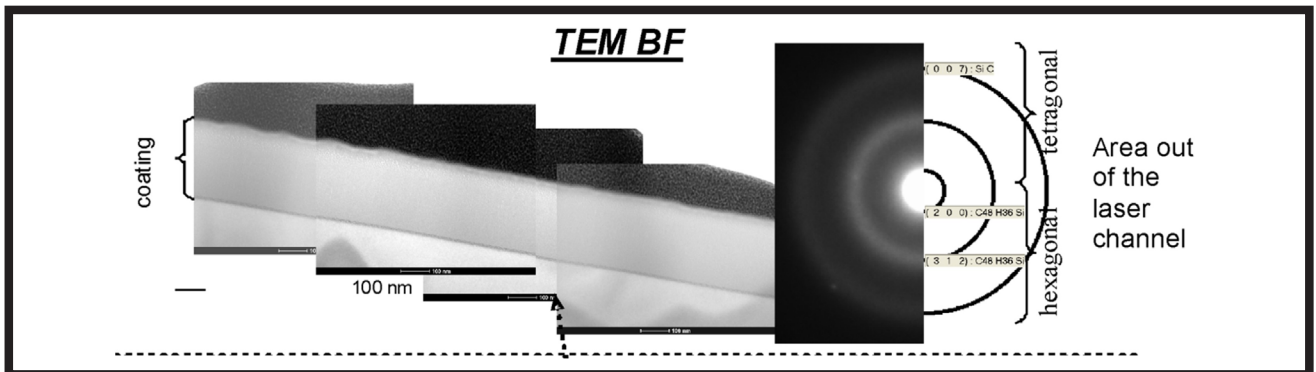


FIG. 5. The TEM microstructure of the area nearby the tubule channel.

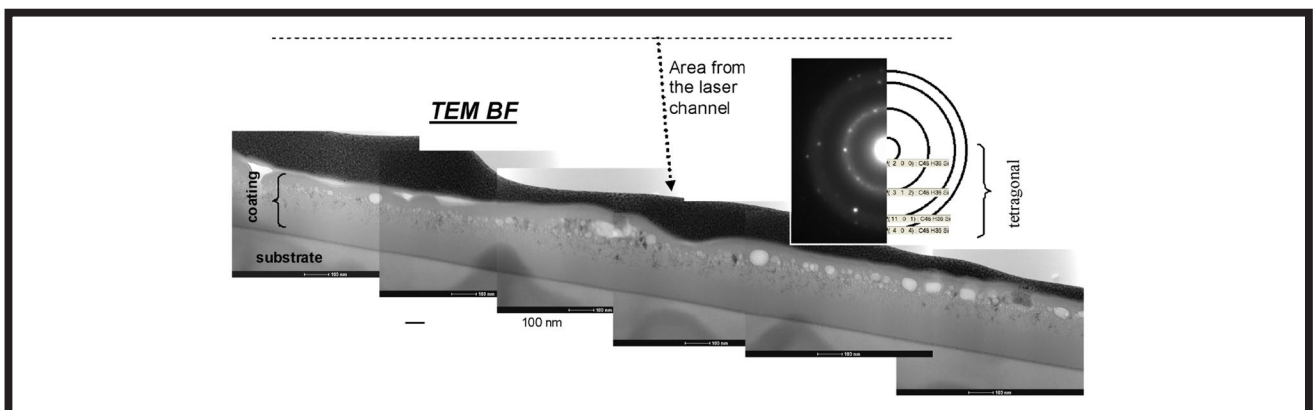


FIG. 6. The TEM microstructure in the tubule channel.

TABLE 5. Results of hemocompatibility tests.

seria	PLT count	conversion into CD61+ objects (i.e. tiles and aggregates combined)				PLT % of all objects	expres- sion PAC-1 [PAC-1 %]	expres- sion P-selectin %+	Platelet leukocyte aggrega- tes (%)
		PLT % of all objects CD61+	PLT-AGR % of all objects CD61+	SMALL PLT-AGG % of all objects CD61+	BIG PLT- AGR % of all objects CD61+				
bas	238.00	95.30	4.70	4.66	0.04	100.00	28.10	1.09	16.57
C225-2		93.87	6.13	6.04	0.09	89.69	30.83	4.42	72.60
C225-4		97.33	2.67	2.64	0.03	72.21	21.23	1.66	60.03
C225-6		97.00	3.00	2.97	0.03	72.26	20.03	1.82	72.43
Kontrola		86.84	13.16	11.24	1.92	67.99	36.07	5.60	39.40
ADP		62.99	37.01	20.84	16.17	20.07	97.47	74.23	16.73

TABLE 6. Tests of hemogliness of coatings of type a-C:H.

Series	Sample	Concentration nMx20
1	Bas (negative control)	8.0
1	C225 2+3	11.7
1	C225 4+5	16.3
1	C225 6+7	9.1
1	Ti	24.9
1	ADP (Positive control)	8.7
2	bas	29.1
2	C225 2+3	38.5
2	C225 4+5	35.9
2	C225 6+7	43.6
2	Ti	42.5
2	ADP	27.5
3	bas	15.4
3	C225 2+3	35.5
3	C225 4+5	20.4
3	C225 6+7	60.0
3	Ti	28.4
3	ADP	18.8

Small and large platelet aggregates were calculated using forward/backward scattering gates for CD61 positive objects. All other chemical compounds were obtained from Sigma-Aldrich. The results of the hemocompatibility studies show the degree of activation and aggregation (TABLE 5).

The thrombogenic potential of blood plasma was measured with the Zymuphen MP activity ELISA test (Hyphen Biomed, Er-agny, France), according to the manufacturer's instructions. This test is based on capturing phospholipid-rich microparticles from cell membranes using immobilized annexin V and then reconstituting the thrombin activity with a solution of calibrated clotting agents. The proteolytic activity of generated thrombin against the chromogenic medium closely correlates with the concentration of microparticles present in blood plasma. The test results are presented in TABLE 6.

Cytotoxicity assessment

Cytotoxicity testing was carried out on the materials selected from the first group and presented in TABLE 2. The tests were performed using human skin fibroblasts (NHDFNHDF) as model cells (purchased from Promocell) which continuously secrete various extracellular matrix components. Depending on their origin and physiological state, fibroblasts may exhibit different morphological phenotypes and different functional properties. Skin fibroblasts are isolated from the dermis of adolescents and adults.

Genotoxicity studies consisted in assessing the effect of the material on the lactate dehydrogenase level by means of the colorimetric method and analysis of microcellular nucleus formation by Luminex.

Cytotoxicity analysis – LDH

Lactate Dehydrogenase (LDH) is an enzyme that is found in the human cells and is involved in glucose metabolism. It easily penetrates the blood serum due to cell death, blood imbalance or increased cell membrane permeability. Its increased level is caused by the cell damage. By measuring the level of the released enzyme, the degree of cell lysis was determined using Lactate Dehydrogenase Activity Assay Kit (purchased from Sigma-Aldrich).

The results of cytotoxicity tests were based on the level of lactate dehydrogenase (LDH) and mutagenic effects on genes encoding characteristic control proteins responsible for the normal cell cycle. The results are shown in FIG. 7.

The given NeA negative control (set) consisted of HeLa cells treated with lambda phosphatase. Lambda Phosphatasephosphatase (Lambda PP) is an Mn^{2+} dependent protein phosphatase with activity against phosphorylated serine, threonine and tyrosine residues. Two positive controls were prepared for the experiment in order to observe the dynamics of activity derived from all possible proteins:

a) Positive control 1 (set) - Jurkata cells treated with 25 μM anisomycin.
b) Positive control 2 (set) - A549 cells treated with 5 μM camptothecin. The cytotoxicity tests results carried out via the LDH release indicate a high level of safety of the tested materials. The results slightly exceed the control level.

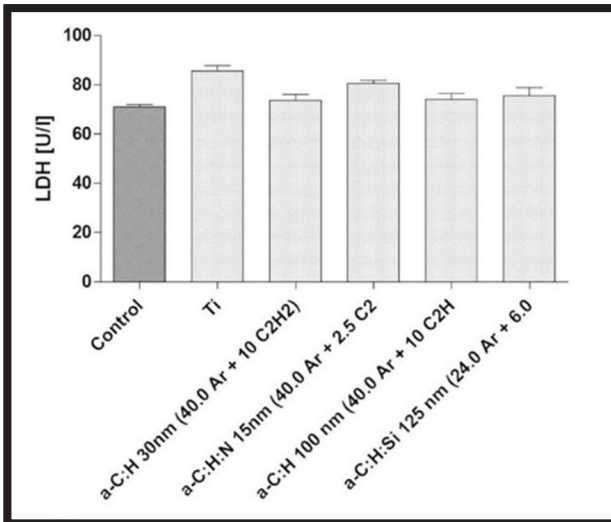


FIG. 7. Results of cytotoxicity assessment lactate dehydrogenase method.

Luminex genotoxicity analysis

MILLIPLEX® MAP is based on Luminex xMAP® technology (purchased from Merck) - one of the most widely accepted multiplexing technologies. This technology is used in life sciences and allows various biological tests, including immunological tests, to be performed on the surface of fluorescent encoded beads, called MagPlex®-C microspheres. Luminex uses its own techniques for internal coding of microspheres using two fluorescent dyes. Due to the precise concentration of these dyes, 100 individually colored sets of beads can be created, each coated with a specific interceptor antibody. After the sample is captured by the analyte, the biotinylated detection antibody is introduced. The reaction mixture is then incubated with streptavidin-PE conjugate, a reporter molecule, to complete the reaction on the surface of each microsphere. The microspheres are illuminated and the internal colorants fluoresce, which means they indicate the set(s) of microspheres used in the test. A second light source induces PE phycoerythrin, a fluorescent dye on the reporter molecule. Fast digital signal processors identify each microsphere and quantify the biological test result from the fluorescent signals of the reporter.

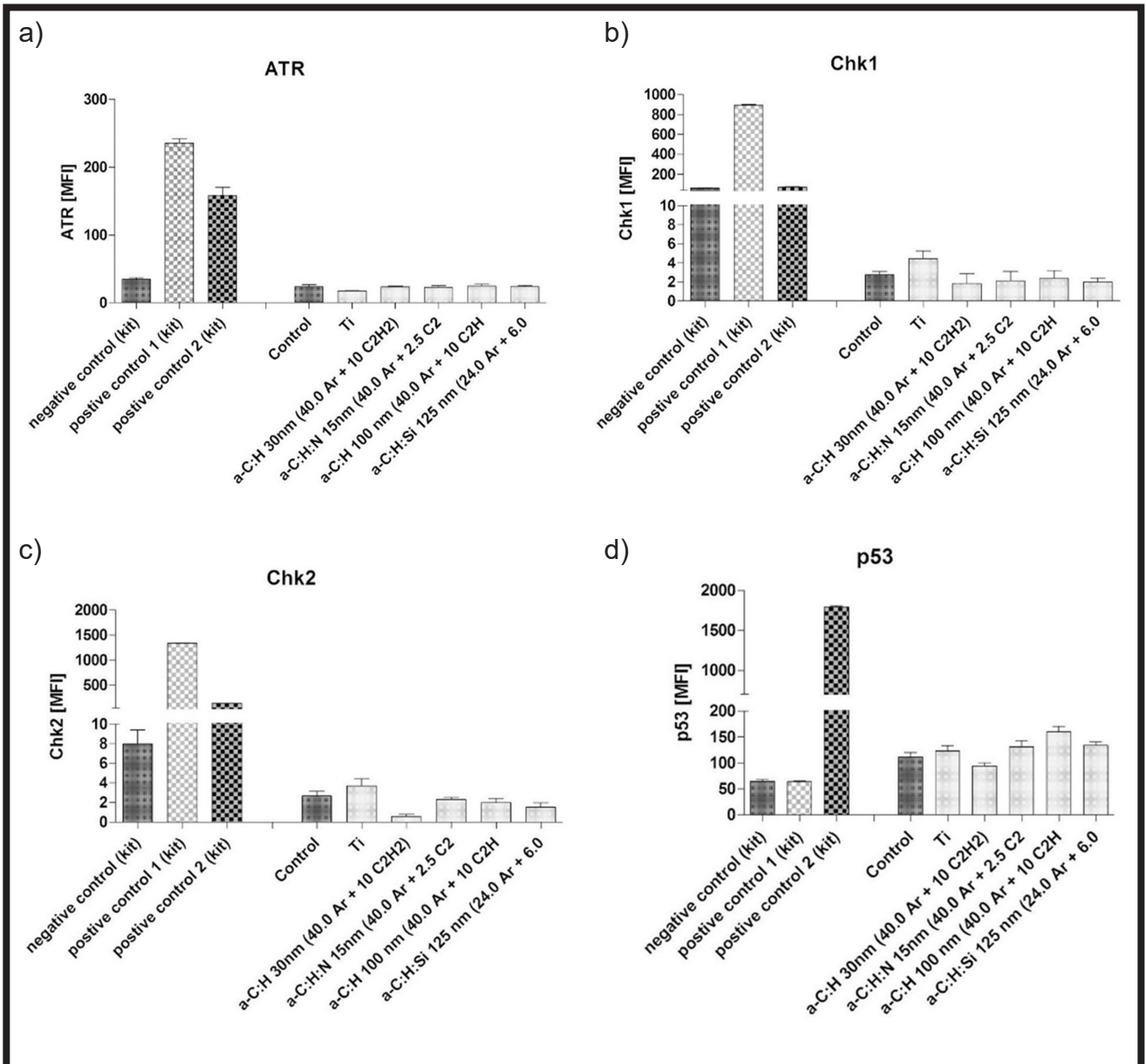


FIG. 8. Results of genotoxicity testing of selected surfaces.

The ability to add multiple conjugated beads to each sample gives the possibility to obtain multiple results for each sample. The open architecture xMAP® technology allows multiplexing of many types of biological tests, reducing time, labor and costs, compared to traditional methods. The following analytes were tested: RANTES, PDGF-AA and PDGF-AB/AA.

Chromatin binding and ataxia telangiectasia and Rad3-related activation (ATR) were observed in the cells treated with replication inhibitors. ATR recognizes replication abnormalities associated with the presence of DNA damage, such as replication forks blocked at the site containing the degradation products. The results are shown in FIG. 8a. No activation of the gene responsible for encoding the ATR protein was found.

Checkpoint 1 kinase, commonly called Chk1, is a human specific serine / threonine / threonine kinase encoded by the CHEK1 gene. Chk1 coordinates the DNA damage response (DDR) and cell cycle checkpoint responses. Activation of the CHK1 gene initiates cell cycle checkpoints, stopping the cell cycle, DNA repair and cell death to prevent damaged cells from passing through the cell cycle (FIG. 8b).

The human gene encoding the CHEK2 protein is an effector kinase involved in DNA repair. CHEK2 is an anticoncogen; its protein product, interacting with the P53 protein, among others, stops the cell cycle. The results are shown in FIG. 8c. A low level was observed for all tested materials, at the control level.

The results of P53 activation are shown in FIG. 8d. In all the diversity and variety of proteins present in living organisms, one protein obtained a special status. The P53 protein, which is also sometimes called “genome guard”. P53 is a protein with transcription factor activity that binds to the DNA in the promoter region and can modulate the expression of many genes, so its effect on activation is crucial. The results of the study indicated the low level of activation of the gene encoding P53 protein.

Surface functionalization via ducts in porous coatings

Migration channels were created on the materials presented in TABLE 2. For cutting out the channels the III harmonic from 355 nm wavelength was used. The laser was coupled with a galvanometer scanner with a telecentric lens of 160 mm focal length. The scanning speed was constant in all the cases and equaled 1 mm/sec. The pulse duration was about 70 ps and the repetition frequency was 1 kHz. The energy of laser pulses ranged from 9 to 10 uJ. The surface functioning was based on the application of coatings on the tubules using the electrostatic influence method. Pol electrolytes were used for surface modification.

Multilayer coatings from polyelectrolyte were made using the so-called “layer by layer” method. In the first stage, a surface charge was generated at TPU to enable anchoring of the first layer of the first polyelectrolyte. The substrate was activated with 10 M NaOH for 25 min and was rinsed with pure Milli-Q water to remove NaOH. Such chemical etching resulted in a negative charge on the substrate surface. At the same time, polycation, i.e. poly-L-lysine (PLL) and polyanion, i.e. hyaluronic acid (HA), were dissolved in 400 mM solution HEPES/0.15 M NaCl with the concentration of 0.5 and 1 mg/ml respectively. The pH of the solutions was adjusted to 7.4 by adding 0.5 M NaOH. After each stage of the deposition, in order to remove excess polyelectrolyte, the samples were rinsed in 0.15 M NaCl buffer solution with pH 7.4. The process was repeated until the desired number of double-layers was reached. PLL was always the outer layer. Finally, the samples were rinsed and stored at 4°C in 400 mM of HEPES/0.15M NaCl buffer solution with pH 7.4.

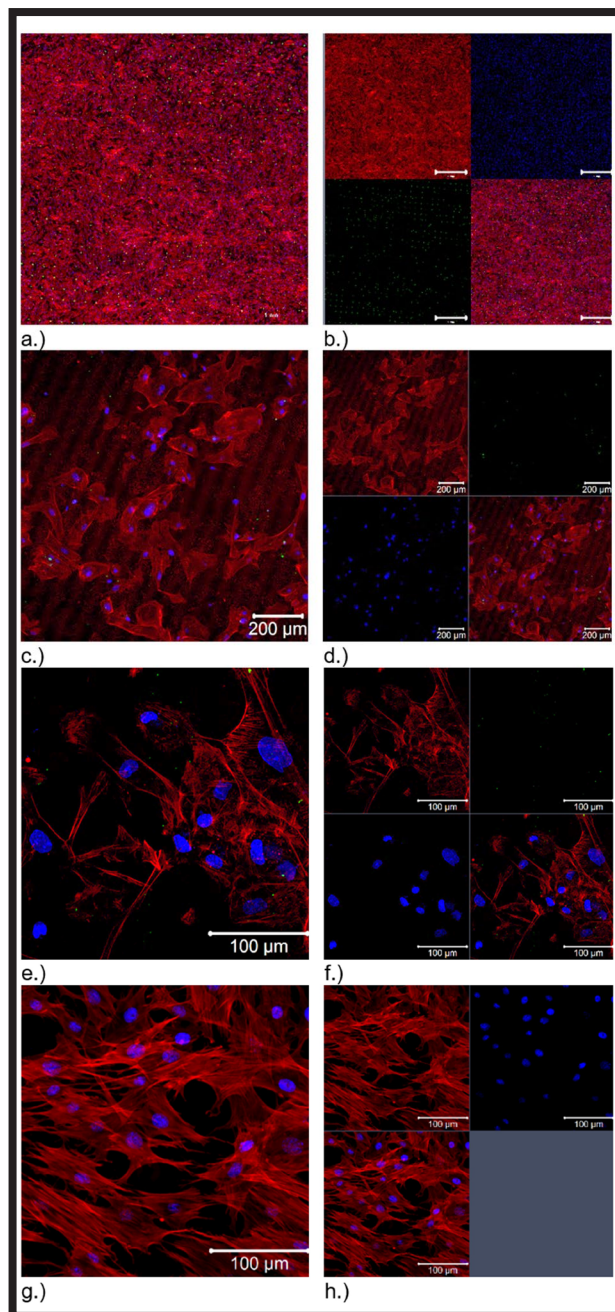


FIG. 9. Cell-material interaction on the surface without structuring.

HUVEC migration studies

Local adhesion and adhesive plaques are membrane bound complexes that serve as nucleation sites for actinic fibres and as connections between cells. They are also places of signal transduction, initiating path signaling in response to adhesion. The Focal Adhesion Staining Kit (FAK100 Catalogue Number) is a very sensitive immunocytochemical tool that contains fluorescent labeled falloidin (conjugated with TRITC) to map the local orientation of actin fibres in a cell and the monoclonal antibody against vinulin, which is very specific for staining focal contacts in cells. The kit also includes DAPI for fluorescent core marking. The results of the tests of the non-structured materials are shown in FIG. 9.

The results of the tests on the structured materials are presented in FIG. 10.

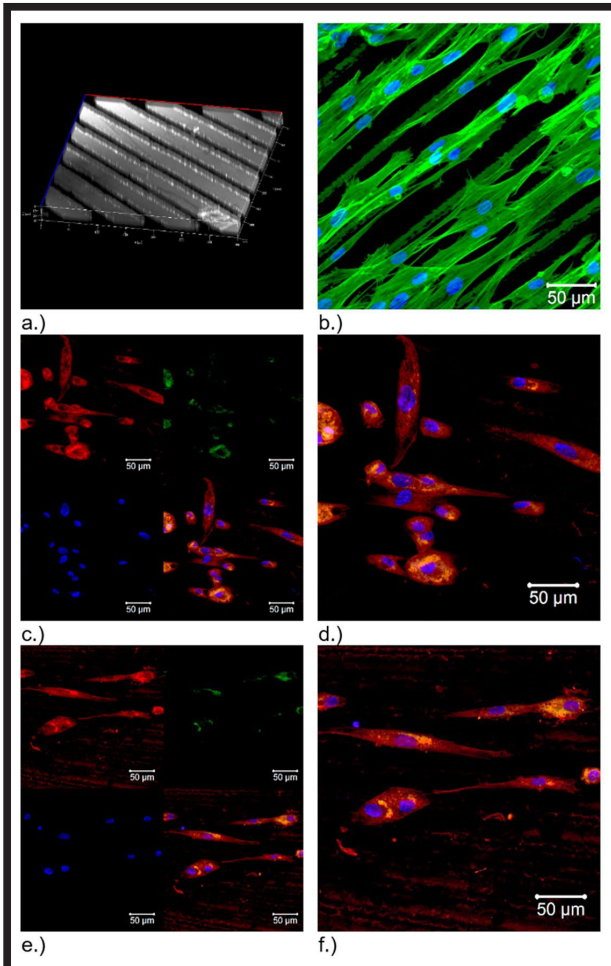


FIG. 10. Cell-surface interaction after surface structuring; a) Topography of migration channels; b) Staining of cytoskeleton actin (green, excitation 488 nm) and nuclei (blue excitation 405 nm) of HUVEC cells on migration channels; c) I place, SPLIT image - Staining: Vinculine monoclonal, maple 7F9, TRITC-guided phloidyne, DAPI; d) II place, full image, FAK 100; e) staining, Second place, SPLIT image - staining: Vinculina monoclonal, 7F9 clone, TRITC-guided phloidyne, DAPI; f) II place full image, tinting FAK 100.

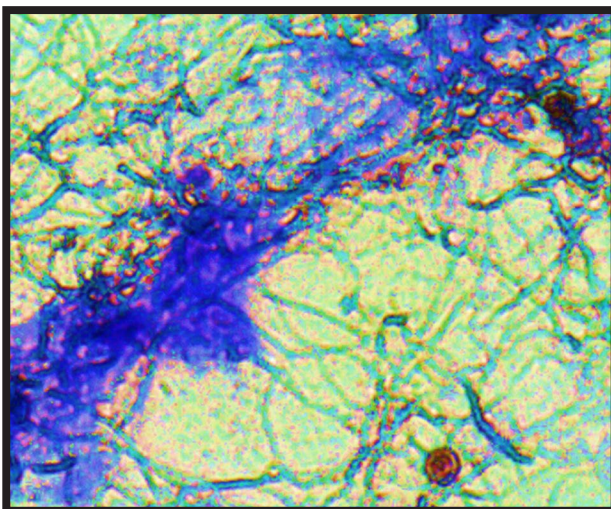


FIG. 11. Preliminary results of revascularization tests.

Discussion

The aim of this work was to develop the material surface facilitating integration with the tissue. The project focused on the surface integration with cardiac tissue and integration with a specific form of connective tissue such as blood. The surface modifications for both issues was performed via laser evaporation of a part of the biocompatible layer, creating a suitable environment for a specific tissue. The interaction of the cells with the material is strictly dependent on such surface properties as: topography, microstructure or mechanical properties. In the case of integration with the heart endothelium, the metallic surface was enriched with bio- and hemocompatible coatings based on amorphous, hydrogenated carbon. The prepared coatings were additionally modified with silicon and nitrogen. These surfaces underwent further modification - patterns made by laser nanolithography. This technique determines the high precision of the shape, size and distribution of the patterns. Periodisation of the surface provided an optimal surface and pattern suitable for cell adhesion and proliferation processes. In the project, an attempt was made to produce normal blood vessels on the network surfaces. We attempted to produce the network of blood vessels through polymeric polyelectrolyte coatings and to control proteins and proangiogenic factors. The conducted experiments gave positive results, however, it was not possible to obtain the appropriate repeatability. Further studies are recommended.

Conclusions






The following goals were achieved in the course of the work:

- ultra-thin amorphous carbon coatings (a-C:H) on Ti and Ti6Al4V substrates of varying thickness, applied using physical techniques from the gaseous phase
- description of the influence of coating application parameters on the hemocompatibility of the surface
- specific properties of the materials in terms of cytotoxicity and genotoxicity
- structured surface with different architecture (2D and 3D structures) and topography obtained and optimized by means of direct laser interference lithography
- characteristics of morphology, topography and mechanical properties of surfaces
- evaluation of protein adsorption (albumin) to the substrate and influence of the protein layer on inhibition of coagulation processes
- description of the influence of surface periodisation on endothelial cell response and blood vessel formation
- the valuable influence of surface nanostructuring on targeted cellular growth and production of adhesion molecules
- the revascularization attempt was not fully successful. Repetitive results were not achieved despite the introduction of VEGF growth factors into polyelectrolyte structures (FIG. 11).

Acknowledgments

The research was financially supported by the statue work Z-2 and Project no. 2016/21/N/ST8/00186 "Functional carbon based coatings on titanium substrate, modified by laser ablation designed for the integration with cardiac tissue and ultimately inhibit the blood clotting process" of the National Science Centre Poland.

ORCID iDs

- R. Major:  <https://orcid.org/0000-0003-3809-1908>
 R. Ostrowski:  <https://orcid.org/0000-0001-7291-2576>
 M. Surmiak:  <https://orcid.org/0000-0001-8396-1488>
 K. Trembecka-Wójciga:  <https://orcid.org/0000-0002-6877-530X>
 J. Lackner:  <https://orcid.org/0000-0003-3931-232X>

References

- [1] Novosel E.C., Kleinhans C., Kluger P.J.: Vascularization is the key challenge in tissue engineering. *Advanced Drug Delivery Reviews* 63 (2011) 300–311.
- [2] Weng Y., Chen J., Tu Q., Li Q., Maitz M.F., Huang N.: Biomimetic modification of metallic cardiovascular biomaterials: from function mimicking to endothelialization in vivo. *Interface Focus* 2 (2012) 356–365.
- [3] Druecke D., Langer S., Lamme E., Pieper J., Ugarkovic M., Steinau H.U., Homann H.H.: Neovascularization of poly(ether ester) blockcopolymer scaffolds in vivo: long-term investigations using intravital fluorescent microscopy. *J. Biomed. Mater. Res. A* 68 (2004) 10–18.
- [4] McGuigan A.P., Sefton M.V.: The influence of biomaterials on endothelial cell thrombogenicity. *Biomaterials* 28 (2007) 2547–2571.
- [5] Bacakova L., Filova E., Parizek M., Ruml T., Svorcik V.: Modulation of cell adhesion, proliferation and differentiation on materials designed for body implants. *Biotechnology Advances* 29 (2011) 739–767.
- [6] Scherthner M., Reisinger B., Wolinski H., Kohlwein S.D., Trantina-Yates A., Fahrner M., Romanin Ch., Itani H., Stifter D., Leitinger G., Groschner K., Heitz J.: Nanopatterned polymer substrates promote endothelial proliferation by initiation of b-catenin transcriptional signaling. *Acta Biomaterialia* 8 (2012) 2953–2962.
- [7] de Mel A., Jell G., Stevens M.M., Seifalian A.M.: Biofunctionalization of biomaterials for accelerated in-situ endothelialization: a review. *Biomacromolecules* 9 (2008) 2969–2979.
- [8] Biggs M.J.P., Richards R.G., Gadegaard N., Wilkinson C.D.W., Oreffo R.O.C., Dalby M.J.: The use of nanoscale topography to modulate the dynamics of adhesion formation in primary osteoblasts and ERK/MAPK signalling in STRO-1+ enriched skeletal stem cells. *Biomaterials* 30 (2009) 5094–5103.
- [9] Guvendiren M., Burdick J.A.: The control of stem cell morphology and differentiation by hydrogel surface wrinkles. *Biomaterials* 31 (2010) 6511–6518.
- [10] Ohl A., Schröder K.: Plasma-induced chemical micropatterning for cell culturing applications: a brief review. *Surf Coat Technol* 116–119 (1999) 820–830.
- [11] Benson R.S.: Use of radiation in biomaterials science. *Nucl Instrum Methods Phys Res B* 191 (2002) 752–757.
- [12] Gumpenberger T., Heitz J., Bäuerle D., Kahr H., Graz I., Romanin C., Svorcik V., Leisch F.: Adhesion and proliferation of human endothelial cells on photochemically modified polytetrafluoroethylene. *Biomaterials* 24 (2003) 5139–5144.
- [13] Kearns V.R., McMurray R.J., Dalby M.J.: Biomaterial surface topography to control cellular response: technologies, cell behaviour and biomedical applications. In: Williams R, editor. *Surface modification of biomaterials*. Oxford: Woodhead Publishing; 2011. p. 169–201.
- [14] Kruss S., Wolfram T., Martin R., Neubauer S., Kessler H., Spatz S.P.: Stimulation of cell adhesion at nanostructured Teflon interfaces. *Adv Mater* 22 (2010) 5499–5506.
- [15] Martínez E., Lagunas A., Mills C.A., Rodríguez-Seguí S., Estévez M., Oberhansl S., Comelles J., Samitier J.: Stem cell differentiation by functionalized micro- and nanostructured surfaces. *Nanomedicine* 4 (2009) 65–82.
- [16] Marczak J.: Micromachining and patterning in micro/nano scale on macroscopic areas. *Archives of Metallurgy and Materials* 6 (2015) 2221–2234.
- [17] Hedberg-Dirk E.L., Martinez U.A.: Large-Scale Protein Arrays Generated with Interferometric Lithography for Spatial Control of Cell-Material Interactions. *Journal of Nanomaterials* (2010) 1–9.
- [18] Tang L., Eaton J.W.: Natural responses to unnatural materials: A molecular mechanism for foreign body reactions. *Mol Med* 5(6) (1999) 351–358.
- [19] Marczak J.: Micromachining and patterning in micro/nano scale on macroscopic areas. *Archives of Metallurgy and Materials* 6 (2015) 2221–2234.
- [20] Sanak M., Jakiela B., Wegrzyn W.: Assessment of hemocompatibility of materials with arterial blood flow by platelet functional tests. *Bulletin of the Polish Academy of Science Technical Science*, 58(2) (2010) 317–322.
- [21] Yi P., Peng L., Huang J.: Multilayered TiAlN films on Ti6Al4V alloy for biomedical applications by closed field unbalanced magnetron sputter ion plating process. *Materials Science and Engineering C* 59 (2016) 669–676.
- [22] Felgueiras H.P., Evans M.D., Migonney V.: Contribution of fibronectin and vitronectin to the adhesion and morphology of MC3T3-E1 osteoblastic cells to poly(NaSS) grafted Ti6Al4V. *Acta Biomaterialia* 28 (2015) 225–233.
- [23] Goodman S.L., Cooper S.L., Albrecht R.M.: The effects of substrate-adsorbed albumin on platelet spreading. *Journal of Biomaterials Science, Polymer Edition* 2 (1991) 147–159.
- [24] Brash J.L., *Macromol. Chem. Suppl.* 9 (1985) 69.
- [25] Lambrecht L.K., Young B.R., Stafford R.E., Park K., Albrecht R.M., Mosher D.F., Cooper S.L.: The influence of preadsorbed canine von Willebrand factor, fibronectin, and fibrinogen on ex vivo artificial surface-induced thrombosis. *Thrombosis Res.* 41 (1986) 99–117.
- [26] Rabe M., Verdes D., Seeger S.: Understanding protein adsorption phenomena at solid surfaces. *Advances in Colloid and Interface Science* 162 (2011) 87–106.
- [27] Vogler E.A.: Protein adsorption in three dimensions. *Biomaterials* 33 (2012) 1201–1237.